Microbes reduce susceptibility of *Aedes aegypti* to Zika virus by enhancing blood digestion and limiting midgut cell infection

William Louie[1], Ana L. Ramírez[1], Lindsey K. Mack[2], Erin Taylor Kelly[2], Geoffrey M. Attardo[2], Lark L. Coffey[1]*

[1]Department of Pathology, Microbiology, and Immunology, School of Veterinary Medicine, University of California Davis, Davis, California, United States

[2]Department of Entomology and Nematology, University of California, Davis, Davis, CA, United States

*Corresponding Author, lcoffey@ucdavis.edu

Short Title: Microbes mediate Zika virus susceptibility in mosquitoes

Abstract

The worldwide expansion of mosquito-borne pathogens necessitates improved control measures, including approaches to restrict infection and transmission by mosquito vectors. Reducing transmission is challenging because determinants of vector competence for viruses like Zika (ZIKV) are poorly understood. Our previous work established that *Aedes (Ae.) aegypti* larvae reared in microbe-rich environmental water are less susceptible to ZIKV as adults compared to cohorts reared in microbe-deficient laboratory tap water. Here, we explain the association by identifying a mechanism by which environment-derived microbes reduce susceptibility of *Ae. aegypti* for ZIKV. Provided that the midgut represents the first barrier to mosquito infection, we hypothesized that microbial exposure modulates midgut infection by

ZIKV. Since mosquitoes live in water as larvae and pupae and then transition to air as adults, we also define the stage in the life of a mosquito when microbial exposure reduces ZIKV susceptibility. *Ae. aegypti* larvae were reared in microbe-rich water and then treated with antibiotics during the pupal and adult stages, adult stage only, or provided no antibiotics at any stage. Vector competence was next evaluated in mosquitoes that ingested ZIKV-spiked bloodmeals. Antibiotic treatment enhanced ZIKV infection and dissemination rates, especially in *Ae. aegypti* treated as both pupae and adults. Antibiotic treated adult mosquitoes also had increased midgut epithelium permeability, higher numbers of ZIKV-infected midgut cells, and impaired bloodmeal digestion. Consistent with these changes, *Ae. aegypti* treated with antibiotics as pupae and adults that ingested ZIKV in bloodmeals showed reduced expression of genes associated with bloodmeal digestion and metabolism relative to mosquitoes that were not antibiotic treated. Together, these data show that exposure to microbes throughout the life of *Ae. aegypti* restricts ZIKV dissemination by facilitating blood digestion and limiting midgut cell infection. Understanding the roles mosquito microbiota play in determining midgut physiology and arbovirus susceptibility can lead to novel approaches to decrease mosquito transmission and will improve understanding of vector competence in microbe-rich environmental habitats.

Author Summary

Mosquito-transmitted viruses like Zika continue to threaten human health. Absent vaccines or treatments, controlling mosquitoes or limiting their ability to transmit viruses represents a primary way to prevent mosquito-borne viral diseases. The role mosquito microbiota play in shaping transmission of Zika virus has been limited to association-based studies. Our prior work showed that *Aedes aegypti* mosquito larvae that develop in bacteria-rich water are less susceptible to Zika virus compared to larvae reared in microbe-poor laboratory tap water. Here we identify a mechanism that explains this association. Since mosquitoes are aquatic as larvae

and pupae and terrestrial as adults, we also define the life stage when microbes need be present to reduce Zika virus susceptibility. We used antibiotics to reduce environmental water-derived microbes at pupal and adult or only adult stages and observed that, compared to mosquitoes with microbes, antibiotic treatment increases Zika virus dissemination, increases permeability and infection of the midgut, and impairs bloodmeal digestion. These data show that microbial exposure throughout the life of a mosquito restricts Zika virus dissemination by facilitating blood digestion and limiting midgut cell infection. These findings advance understanding of microbiota-mosquito-virus interactions by defining how microbes reduce susceptibility of *Aedes aegypti* to Zika virus.

Introduction

Aedes (Ae.) aegypti and *Ae. albopictus* mosquito-transmitted viruses, including dengue (DENV), chikungunya (CHIKV), and Zika (ZIKV), pose a massive burden on human health, especially in tropical regions. Absent licensed vaccines or specific treatments for these pathogens, vector control represents the primary means to reduce the diseases they cause. Vector competence studies, which assess the capacity for mosquitoes to become infected with, develop disseminated infections, and transmit viruses in laboratory environments, are foundational to defining which species maintain arbovirus transmission cycles. For *Ae. aegypti,* prior studies show that temperature (1,2) and geographic origin (3,4) are major determinants of ZIKV vector competence. Other factors, including the microbial environment of mosquito vectors, have historically been overlooked. The microbiota of *Aedes spp.* mosquitoes primarily derive from the environment (5–7), reside dominantly in the midgut (7,8), and can influence physiology and life history traits through nutritional supplementation (5,6,9,10) and immune stimulation (11–13). Prior studies from our group and others' show that microbiota influence ZIKV competence for *Ae. aegypti* (14,15), and *Ae. albopictus* (16). We discovered that when *Ae. aegypti* larvae reared

in microbe-rich water sourced from cemeteries were exposed orally to ZIKV as adults, they became infected, developed disseminated infections, and transmitted virus less efficiently than cohorts where larvae were reared in microbe-deficient laboratory tap water (14). We also determined that the presence of microbes accelerates mosquito development. Another study demonstrated that ablation of microbiota via oral treatment of adult *Ae. aegypti* with antibiotics prior to exposure to ZIKV in an artificial bloodmeal did not affect vector competence (17). Together, these findings suggest that the influence of microbiota on ZIKV vector competence may be specific to the mosquito developmental stage (larval, pupal, adult) during which the microbes are present. Beyond ZIKV, microbial effects on mosquito life-stage development and metabolism that condition pathogen susceptibility may be generalizable to an array of mosquito-borne pathogens. Depending on the bacterial species, larval gut microbiota can modify lipid metabolism in *Ae. aegypti*, including to decrease DENV susceptibility, possibly via metabolism-driven fitness changes (18). Bacterial infection in *Anopheles (An.) gambiae* larvae increases hemocyte activity in adults, which correlates with elevated *Plasmodium falciparum* susceptibility in vectors (19). To understand whether reduced ZIKV vector competence after larval development in microbe-rich water is conferred transstadially from larvae to pupae to adults, one goal of this study was to determine whether exposure to microbes throughout life is required to reduce ZIKV susceptibility in *Ae. aegypti*.

Microbes are likely also involved in maintaining physical barriers that restrict access of an ingested virus or parasite to the mosquito midgut. Treatment of the malaria vector *An. coluzzi* with antibiotics hinders the synthesis of the peritrophic matrix (PM), a chitinous mesh that sequesters the bloodmeal and furnishes digestive enzymes used in bloodmeal digestion (20). Given that the mosquito midgut represents the first infection barrier for most vector-borne pathogens, we hypothesized that microbial exposure affects midgut integrity, which in turn conditions susceptibility to ZIKV. Physiological interactions between microbes and the mosquito

midgut that influence vector competence are supported by prior studies. The commensal bacterium *Serratia marcescens* increases susceptibility of *Ae. aegypti* for CHIKV by secreting a protein that digests membrane-bound mucins coating the gut epithelium, rendering the epithelium more accessible to the virus (21). The bacterium *Bacillus thuringiensis* svar. *israelensis* (Bti) expresses δ-endotoxins that create pores in midgut cells of larval mosquitoes, which is lethal and has been a mainstay of larvicidal vector control for decades (22,23). We predicted that elimination of microbes disrupts midgut integrity, increasing ZIKV access to or traversion of the midgut epithelium, resulting in increased midgut cell infection and higher dissemination rates *Ae. aegypti*. We reared *Ae. aegypti* larvae in microbe-rich environmental water. Half of the experimental cohorts were administered antibiotics in water during the pupal stage to ablate microbes. Some cohorts of adults were also treated with antibiotics administered in sugar water after eclosion and prior to exposure to ZIKV-spiked bloodmeals. We measured physiological differences in the midgut in blood-engorged mosquitoes across cohorts treated with or without antibiotics and treated at different life stages. Microscopy was used to evaluate midgut anatomy and integrity and to quantify ZIKV-infected midgut cells. The magnitude and rate of bloodmeal digestion was measured by quantifying hemoglobin levels. RNA sequencing (RNA seq) was used to identify differential gene expression in cohorts of *Ae. aegypti* treated with or without antibiotics at different life stages and in response to blood with or without ZIKV. We observed that *Ae. aegypti* treated with antibiotics as pupae and adults and as adults only are more susceptible to ZIKV infection and dissemination compared to mosquitoes that were not antibiotic-treated, and that susceptibility is highest after antibiotic exposure at both pupal and adult stages. Antibiotic treatment of pupae and adults also increased midgut permeability, the number of ZIKV-infected midgut cells, and impaired bloodmeal digestion. Gene ontology analyses of ZIKV-exposed mosquitoes revealed enrichment of PM-associated genes, with more genes related to blood protein metabolism upregulated in mosquitoes harboring microbiota. Together our results show that exposure to a microbe-rich community throughout the life of *Ae.*

aegypti facilitates blood digestion which reduces midgut cell infection and restricts ZIKV dissemination.

Materials and Methods

Biosafety

All ZIKV infection experiments were conducted in a biosafety level 3 (BSL3) laboratory and were approved by the University of California, Davis Institutional Biosafety Committee under Biological Use Authorization #R1863.

Mosquito sources

Ae. aegypti mosquitoes colonized from field collections from 2 locations in California were used in this study. Mosquitoes were field-collected in 2016 as larvae (Los Angeles) and eggs (Clovis). Mosquitoes from both locations were maintained for several generations at 26°C, 80% humidity, and a 12 h:12 h light:dark (L:D) cycle with 10% sucrose provided to adults and periodic presentation of sheep blood to stimulate egg laying, as described in our previous study (14). Generation F_{20} or F_{22} mosquitoes were used for these studies.

Mosquito rearing and antibiotic treatments

Microbe source and preparation. Microbes from water collected outdoors in cemeteries were added to water in which *Ae. aegypti* larvae were reared, using an approach detailed in our previous study (14). Briefly, 1 liter (L) of collected water was filtered through a 1 mm mesh to remove large debris, centrifuged at 3000 g to pellet microbes, washed 3 times with sterile 1X phosphate buffered saline (PBS, Thermo Fisher Scientific, Emeryville, CA), and frozen in glycerol at -80°C. Microbe aliquots were thawed at room temperature and placed in laboratory tap water prior to addition of mosquito eggs.

Larval rearing. Mosquito eggs were hatched in 1 L deionized (diH_2O) water spiked with 1 mL of microbes from a glycerol stock aliquot. Approximately 1500 larvae were reared in three pans at a density of ~500 larvae/pan. Each pan contained an agarose plug that was prepared by mixing 1% agarose (Sigma-Aldrich, St. Louis, MO) with pulverized fish food (final concentration of 100 g/L, or 10% [Tetra, Melle, Germany]) and rodent chow (final concentration of 80 g/L, or 8% [Teklad Global 18% Protein Rodent Diet, Envigo, Indianapolis, IN]), which was autoclave-sterilized before casting into 12-well plates. One to 2 plugs were added to larval pans every other day until day 15 post-hatch. Larval trays were kept in environmental growth chambers (Binder, Bohemia, NY) at 26°C, 80% humidity, and a 12 h:12 h L:D cycle.

Antibiotic treatments to pupae and adults. Pupae or adults were divided into three treatments: 1) mosquitoes exposed to antibiotics (Abx) both as **p**upae and **a**dults (AbxPA), 2) mosquitoes exposed to antibiotics as **a**dults (AbxA) only, and 3) mosquitoes not exposed to antibiotics (No Abx), where the latter represents the control group. First, pupae were picked and randomly divided into 2 batches each day. The AbxPA batch of pupae was washed in diH_2O containing an antibiotic cocktail consisting of 50 μg/mL each of penicillin, streptomycin, and kanamycin (Sigma-Aldrich, St. Louis, MO) for 10 minutes before transfer to another water vessel containing fresh antibiotic cocktail. The other batch of pupae, from which the AbxA and No Abx groups were derived, was transferred to a separate cage without washing or antibiotics. Adults in the AbxPA group were maintained on the antibiotic cocktail dissolved in 10% sucrose (Thermo Fisher Scientific, Emeryville, CA) *ad libitum*. Adults in the other batch were initially maintained on filter-sterilized 10% sucrose without antibiotics *ad libitum* until eclosion was complete. Once adults reached a density of ~500, females were aspirated out and transferred in cohorts of 80-120 mosquitoes to 32-ounce plastic containers (Amazon, Seattle, WA) with mesh lids. At this point, the second non-antibiotic treated batch was further divided into two treatments: AbxA was provided 10% sucrose *ad libitum* with the antibiotic cocktail, and No Abx was fed 10% sucrose

ad libitum without the antibiotic cocktail. Adult mosquitoes were maintained at 26°C, 80% humidity, and 12 hour:12 hour L:D cycle throughout the experiment. All mosquitoes were housed in the same incubator. Antibiotic treatment experiments were repeated twice and represented as the “high” and “low” ZIKV dose experiments.

Bacterial quantification by 16S qPCR

We measured the efficacy of antibiotic treatment for removing bacteria from AbxA and AbxAP groups by performing 16S qPCR on larvae, pupae, and adults 3-5 days post-eclosion (dpe) from all groups, as well as in L4 larvae and pupae before antibiotic treatment. DNA from 5 L4 larvae, 5 pre-treatment pupae, 5 No Abx, 10 AbxA, and 10 AbxAP individuals was extracted with the Quick-DNA Tissue/Insect Microprep Kit (Zymo Research, Irvine, CA, USA), according to the manufacturer instructions and eluted in 30 µL elution buffer. Extracted DNA was PCR-amplified in the V3-V4 (24) hypervariable region of the 16S rRNA gene, as previously described (14,24). Quantification of bacteria was performed by SYBR Green Real-Time PCR (Thermo Fisher Scientific, Emeryville, CA) to amplify the 16S rRNA gene in whole mosquitoes. Each sample was tested in technical duplicates. 16S quantities were normalized to an *Ae. aegypti* reference ribosomal protein S17 gene (RPS17) and reported as a 16S:RPS17 ratio (25).

Hemolytic activity

Hematophagous bacteria can directly lyse blood cells and confound hemoglobin digestion measurements. Bacterial isolates from adult female *Ae. aegypti* were screened for hemolytic activity via culturing on agar plates. Individual mosquitoes were homogenized (TissueLyser, Retsch, Haan, Germany) in 500 µL PBS and 40 µL of supernatant was plated on either R2A agar (Sigma-Aldrich, St. Louis, MO) or sheep blood agar plates (Biological Media Services, University of California, Davis School of Veterinary Medicine) for 3 days at 37°C. Up to 10 colonies from each mosquito were streaked on media plates 2-3 additional times to generate

axenic cultures. Resulting colonies were streaked on sheep blood agar at both 30°C and 37°C and screened for clearing zones around colonies over the course of 3 days. The viability of this assay was tested in-house with hemolytic *Streptococcus spp.* isolates from the UC Davis School of Veterinary Medicine.

Virus source and titrations

We used ZIKV strain BR15 (Brazil 2015, SPH2015, GenBank Accession # KU321639), the same strain we used previously for mosquito infection experiments (14). This virus strain was originally isolated from human serum from a patient in Brazil in 2015 and passaged 3 times in Vero cells (CCL-81, ATCC, Manassas, VA) before freezing in stocks. Stocks were titrated on Vero cells prior to bloodmeal presentation to approximate stock titers, and ZIKV-spiked sheep blood was also titrated after bloodfeeding to confirm the dose presented in each bloodmeal. For titrations, serial 10-fold dilutions of cell culture supernatant containing virus stock or ZIKV-spiked blood were inoculated into multi-well plates containing confluent Vero cells at one dilution per well and incubated for 1 hour at 37°C in 5% CO_2 with rocking every 10 minutes. After incubation, each well was filled with an agar overlay (0.5% agarose [Thermo Fisher Scientific, Emeryville, CA] in Dulbecco's modified Eagle's medium [DMEM, Thermo Fisher Scientific, Emeryville, CA], + 2% fetal bovine serum [FBS, Genesee Scientific, San Diego, CA] + penicillin/streptomycin [Thermo Fisher Scientific, Emeryville, CA]). The cells were incubated for 1 week at 37°C in 5% CO_2, then fixed with 4% formalin (Thermo Fisher Scientific, Emeryville, CA). Fixed cells were stained with 0.025% crystal violet (Thermo Fisher Scientific, Emeryville, CA) in 20% ethanol and visualized on a light table to count plaques. ZIKV bloodmeal titers are represented as plaque-forming units (PFU) per mL of blood.

ZIKV vector competence experiments

Stock ZIKV in DMEM, or DMEM with no virus as a control, were diluted in 10-fold increments with fresh heparinized sheep blood (HemoStat Laboratories, Dixon, CA) to achieve ZIKV titers of 10^4 and 10^6 PFU/mL. Bloodmeals were presented to female *Ae. aegypti* at 3-5 days post-eclosion in cohorts of 80-120 per container, at 2-3 containers per treatment. Cohort sizes were very large to maximize the numbers of bloodfed mosquitoes in the case of low feeding rates. Mosquitoes were sucrose-starved 18-24 hours before the presentation of bloodmeals. Mosquitoes were offered bloodmeals for 60 minutes through a collagen membrane rubbed with an artificial human scent (BG-Sweetscent mosquito attractant, Biogents USA) and heated to 37°C in a membrane feeder (Hemotek Limited, Blackburn, United Kingdom). Bloodmeals were presented to mosquitoes inside a plexiglass glove box containing an open bottle of boiling water to maximize humidity. After feeding, mosquitoes were immobilized with CO_2 for 5 seconds and then immobilized on a chill table (Bioquip (R.I.P.), Compton, CA, USA) to assess their bloodfeeding status using a microscope at 10X magnification. Fully engorged females (18-45 per treatment for each experiment) were sorted into fresh plastic containers at a density of 10-20 mosquitoes per container and held at 28°C with 80% humidity and 12 h:12 h L:D cycle for 14 days. No Abx cohorts were provided 10% sucrose *ad libitum,* while AbxPA and AbxA cohorts were maintained on 10% sucrose with the antibiotic cocktail *ad libitum*.

At 14 days post-bloodfeed (dpf), surviving mosquitoes were CO_2-anesthetized and immobilized on a chill table. Bodies, legs/wings, and saliva were collected to assess infection, dissemination, and transmission rates, respectively. Legs/wings were removed before collection of expectorate into capillary tubes containing PBS by forced salivation, using an established approach (26). To minimize cross-contamination, surgical tools were washed once in CaviCide® (Metrex, Orange, CA) and twice in 70% ethanol between dissections. Each capillary tube was placed in a 1.5-mL tube containing 250 µL PBS and pulse-centrifuged at 8,000 g to recover saliva. Bodies and legs/wings were placed into 2-mL tubes containing 500 µL PBS and a 5-mm glass bead

(Thermo Fisher Scientific, Emeryville, CA), then homogenized at 30 hertz for 5 minutes in a TissueLyser (Retsch, Haan, Germany). Viral RNA was extracted using a MagMax Viral RNA Extraction Kit (Thermo Fisher Scientific, Emeryville, CA), into 60 µL elution buffer following the manufacturer's recommendations.

Detection and quantification of viral RNA in mosquito tissues and saliva were performed by quantitative reverse transcription polymerase chain reaction (RT-qPCR) using a TaqMan Fast Virus 1-Step Master Mix and a ZIKV-specific primer set (ZIKV 1086F/1162c, probe: ZIKV 1107-FAM) using established methodologies (26,27). Cycle threshold (Ct) values from the RT-qPCR were converted to RNA genome copies using standard curves established with ZIKV RNA of known concentration. Each sample was assayed in technical duplicates and converted to copies per mosquito before calculating the average value. The limit of detection (LOD) was calculated from the standard curve linear regression line where the Ct value = 40. Samples that did not yield a detectable Ct of less than 40 were reported at the LOD. Infection, dissemination, and transmission rates are all reported as the number of ZIKV-positive individuals in their respective tissues divided by the number that ingested ZIKV-spiked blood.

Midgut permeability assessments

A low molecular weight dextran-FITC (MW 4000, Sigma-Aldrich, St. Louis, MO) was co-spiked into ZIKV-bloodmeals and used to measure midgut permeability in No Abx, AbxA, and AbxPA, groups. Permeability was assessed by measuring the fluorescent intensity of dextran-FITC inside versus outside at three locations in the midgut for each mosquito for a total of 5 mosquitoes per treatment. A stock solution of 20 µg/mL dextran-FITC dissolved in PBS was spiked into sheep blood at a 1:20 dilution to achieve 1 µg/mL, the concentration used in a previous study (28). Dextran-spiked blood mixed with 10^5 PFU/ml ZIKV and presented to mosquitoes as described above for vector competence assessments. Blood-engorged

mosquitoes were visualized by fluorescence microscopy to detect FITC in tissues. Samples were covered in foil for all post-dissection steps to minimize photobleaching. Quantification of FITC fluorescence was then performed on Fiji (ImageJ) (29) by measuring intensity relative to background by subtracting fluorescence of an equal-sized region outside the sample area. Fluorescence intensity ratios between the gut lumen and hemocoel were calculated at three randomly drawn areas of equal size around the gut perimeter, then averaged together. Each average was also conducted across three slices per sample to minimize focal plane variation in fluorescence.

Fluorescence imaging of mosquito midguts

Mosquitoes in No Abx, AbxA, and AbxPA groups that ingested ZIKV-spiked bloodmeals were imaged using immunofluorescence microscopy to examine midgut structure and to quantify the number of ZIKV-infected midgut epithelial cells. Legless and wingless mosquito bodies or dissected midguts were placed in 10% formalin in PBS for 24 hours, then prepared for various image-based assessments as described below. Mosquitoes were imaged at the University of California, Davis Advanced Imaging Facility using a Leica TCS SP8 STED 3X inverted microscope.

Midgut structure: Mosquito bodies were washed once in PBS, submerged in PBS with 30% sucrose overnight, and then molded and frozen at -80°C in Tissue Plus OCT medium (Thermo Fisher Scientific, Emeryville, CA). Tissue molds were cut into 10 µm slices at the median sagittal plane (at a depth where the blood bolus reaches maximum diameter, determined with test samples) using a Leica CM1860 Cryostat Microtome (Leica Biosystems, Deer Park, IL, USA) and embedded onto charged microscope slides. A single drop of ProLong Gold Antifade Mountant with DAPI (Thermo Fisher Scientific, Emeryville, CA) was used to mount each slide.

ZIKV-infection of midguts: Dissected midguts in 10% formalin were washed twice in PBS. Tissues were submerged in a blocking solution consisting of 1X PBS, 0.2% Triton X-100

(PBS+T) (Bio-Rad Laboratories, Hercules, CA), 1% bovine serum albumin (BSA, Sigma-Aldrich, St. Louis, MO), and 10% normal goat serum (Lampire Biological Laboratories, Pipersville, PA) for 10 minutes before staining with a primary monoclonal antibody that reacts with multiple flaviviruses (Flavivirus treatment antigen antibody D1-4G2-4-15, Novus Biologicals, Littleton, CO) at a 1:1000 dilution in blocking solution at 4°C overnight. Midguts were washed five times via direct tube transfer in PBS+T before staining with the secondary antibody (Goat anti-mouse Alexa Fluor 594, Abcam, Cambridge, United Kingdom) at a 1:1000 dilution in blocking solution for 1 hour at room temperature. Midguts were washed 5X in PBS+T before mounting onto microscope slides with ProLong Gold Antifade Mountant with DAPI. ZIKV detection and quantification were done by manually counting distinct red patches, using blue DAPI as a reference for individual cells across three slices of a single midgut, and averaging the values. FITC, DAPI, and Alexa Fluor 594 were each visualized (and FITC was quantified) in their respective channels before merging.

Histologic analyses

Histological images at 20X and 40X magnification were used to visualize mosquito anatomy and to validate that sample preparation for immunofluorescence microscopy did not mechanically disrupt the midgut, which could affect interpretations of midgut integrity. Blood-engorged mosquitoes with their legs and wings removed were placed in 10% formalin in PBS for 24 h, then encased within tissue cassettes (Thermo Fisher Scientific, Emeryville, CA) submerged in 70% ethanol. Samples were submitted to the University of California, Davis School of Veterinary Medicine Anatomic Pathology Service, where whole mosquitoes were paraffin-embedded, cut into 5 µm slices, and stained with hematoxylin and eosin (H&E). Slides were visualized at 20X and 40X magnification under a Zeiss Axio Vert A1 inverted light microscope connected to an Axiocam 208 color camera (Carl Zeiss, Jena, Germany). Although we evaluated sections from 5 individual mosquitoes each for No Abx, AbxA, and AbxPA, groups, we used histology readouts

as a qualitative approach to evaluate gross midgut anatomy. Anatomical structures were identified by an expert in mosquito anatomy. Representative images for each of the three groups are shown.

Blood digestion analyses

Quantification of hemoglobin in bloodfed mosquitoes using a hemoglobin colorimetric detection kit (Thermo Fisher Scientific, Emeryville, CA) was used to measure blood digestion. At 0, 1, 2, or 3 dpf, 10-12 individual mosquitoes each in No Abx, AbxA, and AbxPA, groups exposed to blood only or ZIKV-spiked blood with their legs/wings removed were homogenized in 300 µL hemoglobin diluent, 100 µL of which was used for the assay, per manufacturer's instructions. Absorbance at 570 nm was measured from each sample once in 96-well plates using a SpectraMax iD5 Multimode Microplate Reader (Molecular Devices, San Jose, CA). Absorbance values were converted to hemoglobin concentrations via standard curves generated from hemoglobin standards and serial dilutions of fresh sheep blood used for feeding. Output absorbance values were normalized to homogenized, non-bloodfed mosquito negative controls, and units were converted to µg per mosquito body. Before conducting the assay, we validated and optimized this kit for bloodfed mosquitoes, including ensuring that heat incubation of mosquitoes at 60°C for 10 minutes to destroy ZIKV infectivity did not affect hemoglobin quantification (**Figure S1**).

RNA sequencing and bioinformatics

Mosquito messenger RNA was sequenced to determine differences in gene expression associated with antibiotic treatments after ZIKV exposure. Total RNA was extracted from adult female mosquitoes in triplicate pools of 5 individuals each for No Abx, AbxA, and AbxPA groups using the Quick-RNA Tissue/Insect Microprep kit (Zymo Research, Irvine, CA, USA). RNA extracts were eluted into 20 µL elution buffer and quantified using a Qubit fluorometer RNA

high-sensitivity (HS) assay (Thermo Fisher Scientific, Emeryville, CA). Approximately 1 µg of total RNA per sample was submitted to Genewiz Inc. from Azenta Life Sciences (Chelmsford, MA, USA), where poly-A selection, library preparation, and paired-end Illumina HiSeq 2x150 bp were performed. Raw FASTQ data files were received and treated by filtering and trimming reads with *cutadapt v3.2* (30) using default parameters (Quality cutoff >= 30, minimum length of 100 bp). Next, *FastQC* (31) was used to visualize quality scores. Processed reads were then aligned to version AaegL5.2 of an *Ae. aegypti* transcriptome obtained from VectorBase (32) using *bowtie2 v2.4.3* (33). Aligned reads were imported into R and analyzed with the package Differential Expression Analysis using *DESeq2 v1.28.1* (34). Default parameters were used to determine the differential abundance of each gene using an input experimental design of [antibiotic treatment + bloodmeal status + interaction]. Genes with a significance (adjusted P value) below 0.05 are reported. Significant genes were mapped to biological processes using the Gene Ontology program *topGO* (35).

Statistical analyses

The 16S:RPS17 ratios to verify antibiotic efficacy from qPCR were compared using a Kruskal-Wallis test with multiple comparisons for adult mosquito treatments and across life stages. Differences in ZIKV infection, dissemination, and transmission rates between antibiotic-treated groups were determined using Fisher's exact tests. Differences in ZIKV RNA levels in bodies, legs/wings, and saliva across antibiotic-treated groups were assessed by Kolmogorov-Smirnov tests. Differences in hemoglobin levels across antibiotic-treated groups were evaluated using Kruskal-Wallis tests with repeated measures. Relative fluorescence values and numbers of nuclei were averaged in triplicate and tested for significance by one-way ANOVA tests. Differences in numbers of ZIKV-infected midgut epithelial cells were assessed using Fisher's exact tests. For RNA-Seq, statistical tests built into the *DESeq2* package were used. In short, each sample was normalized by library size, and the geometric mean for each gene was

calculated. Negative binomial generalized linear models (glm) were used for each gene to determine differential expression across antibiotic-treated groups. The Wald test was used for statistical significance, with correction for the false discovery rate (FDR) set to 0.05. For principal components analyses (PCA), variance stabilized transformation was implemented before plotting. All statistical analyses, except RNA-Seq, were performed using GraphPad PRISM 9.0.2 (GraphPad Software, San Diego, CA). RNA-Seq analyses were conducted in R *v3.6* (36). P-values of less than 0.05 were considered statistically significant. For gene ontology (GO), Fisher's exact tests were used on GO terms and corrected for the false discovery rate.

Accession number(s). Raw sequencing data are available from the NCBI Sequence Read Archive under BioProject entry PRJNA818687. Scripts for the RNA-Seq analysis are available on Github (DOI: 10.5281/zenodo.7259822).

Results

Reduced *Ae. aegypti* susceptibility to ZIKV conferred by microbial exposure is life stage-dependent

To understand whether reduced ZIKV vector competence after larval development in microbe-rich water that we observed previously (14) is conferred transstadially from larvae to pupae to adults, one goal of this study was to determine whether exposure to microbes throughout life (i.e. at larval, pupal, and adult stages) is required to reduce susceptibility of *Ae. aegypti* to ZIKV. *Ae. aegypti* larvae were reared in laboratory water spiked with microbe-rich water sampled from cemeteries that we characterized in a previous study (14) and was dominated by over 1000 bacterial species from the phyla *Bacteroides*, *Firmicutes*, and *Proteobacteria*. Control mosquitoes were not provided antibiotics (No Abx) at any life stage. To assess the effects of microbe depletion at pupal and adult life stages, cohorts of **p**upae and the **a**dults they

developed into were administered an antibiotic (Abx) cocktail (AbxPA) that was provided to pupae in water and orally in sucrose to adults from eclosion to 3 days of age (**Figure 1A**). To study the effects of antibiotic treatment on adult mosquitoes, we also included cohorts where **a**dults were provided antibiotics (AbxA) orally for 3-5 days post-eclosion. AbxA mosquitoes were not antibiotic-treated before 3 days of age. After each treatment, mosquitoes were orally presented 3-5 days post-eclosion with low or high-dose ZIKV-spiked bloodmeals for vector competence assessments. To maximize bloodfeeding success, sugar with and without antibiotics was withdrawn from mosquitoes 24 hours prior to bloodmeal presentation. We first assessed the efficacy of antibiotic treatment via qPCR quantification of 16S DNA. Antibiotics significantly reduced the number of prokaryotes in all treated groups. (Kruskal-Wallis [K-W] with multiple comparisons, P = 0.002 between No Abx and AbxA [adj. P = 0.002] and No Abx and AbxPA [adj. P = 0.006]) (**Figure 1B**). Significantly higher 16S:RPS17 ratios, our proxy for prokaryote levels, were observed in No Abx L4 larvae and pupae relative to adult mosquitoes (K-W multiple comparisons, P = <0.0001 between No Abx and larva [adj. P = 0.0012] and No Abx and pupa [adj. P = 0.0079]). This is consistent with ours (14) and others' (6,12) previous observations that microbial abundance decreases during mosquito development. Antibiotic treatment of pupae and adults significantly increased ZIKV infection and dissemination rates at both low (3.2×10^4) and high (4.8×10^6) PFU/ml ZIKV bloodmeal doses compared to no antibiotic treatment (Fisher's exact test, infection: P < 0.0001, dissemination: P < 0.0001). Although it increased infection rates, antibiotic treatment of adults did not significantly increase dissemination rates compared to no antibiotic treatment (Fisher's exact test, infection: P = 0.067, dissemination: P = 0.71) (**Figure 1C**). The AbxPA mosquitoes exhibited a more robust dose response to infection, achieving larger increases in rates of infection and dissemination compared to No Abx and AbxA across the two ZIKV doses (**Figure 1D**). Despite increased infection and dissemination rates, transmission rates across antibiotic treatments and at the two ZIKV doses did not differ significantly. Even though transmission rates were not different, levels

of ZIKV RNA levels in saliva were higher in AbxPA compared to AbxA (Kolmogorov-Smirnov test, P = 0.009) at the higher dose, but not higher than No Abx (Kolmogorov-Smirnov test, P = 0.71) (**Figure 1E-F**). These results show that antibiotic treatment during both pupal and adult life stages increases rates of ZIKV infection and dissemination, transmitted titers, and susceptibility to higher ingested doses. These data also reveal that microbes acquired by larvae must be maintained as pupae to reduce ZIKV susceptibility. The observation that antibiotic treatment of adult mosquitoes is not sufficient to enhance ZIKV dissemination suggests that microbe-mosquito interactions that influence ZIKV susceptibility must occur in the aqueous phase of a mosquito's life.

Antibiotic treatment increases midgut permeability

To understand how microbial exposure of larvae and pupae reduce susceptibility of *Ae. aegypti* to ZIKV, we next evaluated midgut integrity. Our rationale for focusing on the midgut is that it represents the first barrier to infection of *Ae. aegypti* by ZIKV after oral exposure. We asked whether higher infection and dissemination rates in AbxPA and AbxA groups compared to the No Abx group are explained by modified epithelial structure or reduced midgut integrity resulting from microbe depletion. We first assessed permeability by directly visualizing and enumerating midgut epithelial cell density in DAPI-stained sections. As a second step, we added FITC-dextran (which is small enough that it can traverse cell membranes) into ZIKV-spiked bloodmeals to visualize and quantify the relative fluorescent intensity of the marker inside versus outside the midgut, where higher fluorescence inside versus outside is indicative of higher midgut integrity. We compared fluorescent intensity across antibiotic-treated groups immediately after ingestion of a bloodmeal with ZIKV (**Figure 2A**). The midgut epithelium was less organized, as evidenced by reduced contiguity in DAPI-stained midgut epithelial cell nuclei in both AbxA and AbxPA compared to No Abx groups (**Figure 2B**). These qualitative observations of structural disorganization of the midgut were also supported quantitatively,

where fewer cells in a 100 μm length of midgut epithelium were detected in AbxPA compared to No Abx groups (**Figure 2C**, P = 0.078). For this assessment, five mosquitoes were examined per group, and three separate sections for each mosquito were randomly selected, quantified, and averaged (**Figure 2D**). The relative dextran-FITC fluorescence inside versus outside of the midgut lumen for the AbxPA group was significantly lower than the No Abx group (P = 0.009), and the AbxA group trended lower (although not significantly) than the No Abx group, indicating that antibiotic treatment increases midgut permeability (**Figure 2E**). To rule out physical rupture or other disruptions to the midgut during sample preparation that may have reduced structural integrity, we treated and stained midgut sections from a separate cohort of similarly treated mosquitoes with DAPI or H&E. At 10X, 20X, and 40X magnification, midgut epithelia across treatments did not appear structurally different (**Figures 2G**, **S1**). Together these data support antibiotic treatment, especially of both pupal and adult *Ae. aegypti* life stages, increasing midgut permeability in adult mosquitoes after ingestion of ZIKV-spiked bloodmeals.

Antibiotic treatment increases ZIKV infection of the midgut epithelium

Next, we asked whether disruptions to midgut integrity with antibiotic treatment translate to greater infection success, measured as higher numbers of ZIKV-infected midgut epithelial cells. We detected ZIKV in midguts by staining sections with a flavivirus binding antibody 2 or 3 dpf and counting the total number of cells in each midgut that were stained with fluorescent anti-ZIKV antibody (**Figure 2A**). The number of ZIKV-positive cells in midguts was significantly higher in the AbxPA group compared to the No Abx group (Brown-Forsythe ANOVA test with Dunnett's multiple comparisons test, P = 0.048, AbxPA versus No Abx P = 0.086) (**Figure 2F**). At 3 dpf, more infected cells were visible in AbxPA compared to AbxA and No Abx (**Figure 2G**). These data support the role of microbes in larvae and pupae in maintaining the integrity of the mosquito midgut, which in turn reduces the susceptibility of the midgut epithelium to infection by ZIKV.

Microbial disruption via antibiotic treatment impairs blood digestion

Since midgut integrity can affect physiology of blood digestion in addition to ZIKV susceptibility, we next assessed whether elevated midgut permeability after antibiotic treatment affects blood digestion. We employed a commercially available hemoglobin colorimetric assay as a proxy for blood protein digestion by quantifying the reduction of hemoglobin levels in blood-engorged mosquitoes on 1 and 2 dpf compared to immediately after feeding on 0 dpf. Before performing the assay, which is typically used for human blood, we first validated and optimized the approach for use with homogenized mosquitoes that ingested sheep bloodmeals. We observed that sheep blood absorbance varies linearly as a function of hemoglobin concentration, like the kit standard (**Figure S2A**) and that absorbance decreases reproducibly in serially diluted mosquitoes at both 560 and 580 nm wavelengths. The assay was unaffected by the 10 minute 60°C heat treatment of homogenized fed mosquitoes used to inactivate ZIKV infectivity in the samples (**Figure S2B**). Blood-engorged females were homogenized and assayed for hemoglobin immediately after bloodfeeding at 0 dpf to assess whether different groups ingested the same bloodmeal volume, as well to measure the kinetics of bloodmeal digestion 1, 2, and 3 dpf (**Figure 3A**). Although hemoglobin levels that approximate bloodmeal size varied in individual mosquitoes, there was no significant difference in mean ingested hemoglobin levels on 0 dpf across antibiotic-treated groups regardless of whether the bloodmeal contained ZIKV, which shows that antibiotic treatment did not influence bloodmeal size (K-W test with multiple comparisons, P = 0.522) (**Figure 3B, C**). After ingestion of blood without ZIKV, mean hemoglobin levels in the AbxPA group were higher than in the No Abx group 2 dpf (K-W test, P = 0.0063). By 3 dpf, mean hemoglobin levels in the AbxPA group were higher than both AbxA and No Abx groups (K-W test with multiple comparisons, adjusted $P_{AbxPA\text{-}No\ Abx}$ = 0.0347, adjusted $P_{AbxPA\text{-}AbxA}$ = 0.051) (**Figure 3B**). The same pattern was observed after ingestion of blood with ZIKV: AbxPA showed a reduced rate of blood digestion compared to No Abx 1 dpf

(K-W test with multiple comparisons, adjusted $P_{AbxPA\text{-}No\ Abx}$ = 0.0368, adjusted $P_{AbxPA\text{-}AbxA}$ = 0.0035) and both No Abx and AbxA 2 dpf (K-W test with multiple comparisons, adjusted $P_{AbxPA\text{-}No\ Abx}$ = 0.0037, adjusted $P_{AbxPA\text{-}AbxA}$ = 0.0027) (**Figure 3C**). The 3 dpf time point for individuals that ingested blood with ZIKV was not assayed for hemoglobin since uneven bloodfeeding rates across cohorts and the desire to maintain statistically robust group sizes led us to prioritize use of 3 dpf mosquitoes for infection and dissemination assessments. We also compared mean hemoglobin levels across treatments and days post-feed for mosquitoes that ingested blood with or without ZIKV. Although levels did not differ immediately after bloodmeal ingestion on 0 dpf, mean hemoglobin digestion was significantly faster in No Abx and AbxA on 1 dpf (K-W test, $P_{No\ Abx}$ = 0.0163, P_{AbxA} = 0.0009) but not AbxPA (K-W test, P = 0.25) in ZIKV-exposed mosquitoes compared to mosquitoes that ingested blood without ZIKV (**Figure 3D**). These data show that ablation of larval and pupal microbes reduce bloodmeal digestion, and that blood with ZIKV is digested more quickly than blood lacking virus.

Reduced bloodmeal digestion promotes susceptibility of *Ae. aegypti* ZIKV dissemination out of the midgut

We hypothesize that, in addition to disrupting midgut cell integrity, antibiotic mediated reduction of microbes in mosquitoes via reduced bloodmeal digestion provides the virus more time to bind and enter midgut epithelial cells, manifest as increased ZIKV infection and dissemination. Increased magnitude of ZIKV dissemination in antibiotic-treated groups was confirmed by measuring ZIKV RNA levels in legs/wings from mosquitoes from each treatment that ingested ZIKV-spiked blood 3 days earlier. The rates of ZIKV dissemination were marginally higher in the AbxPA group (33%) compared to the AbxA (16%) and No Abx (11%) groups (Fisher's exact test, P = 0.06) (**Figure 3E**). In contrast to No Abx and AbxA, all ZIKV-infected individuals in AbxPA also had disseminated infections. To determine whether bacteria with hemolytic activity contribute to bloodmeal digestion in the No Abx groups, bacteria from 5 No Abx treated adult

mosquitoes were cultured on two types of agar and then Sanger sequenced. Although different species of bacteria were detected, none showed hemolytic activity (**Table S1**), suggesting that bloodmeal digestion is not directly mediated by bacteria in the mosquito midgut. Together, these data show that microbes enhance the ability of *Ae. aegypti* to digest blood, likely via an indirect mechanism since the culturable bacteria recovered from mosquitoes that were not antibiotic treated were not hemolytic. The increased rate of blood digestion in mosquitoes with an intact microbiome reduces ZIKV susceptibility.

Microbial promotion of bloodmeal digestion and reduction in ZIKV susceptibility is manifest across genetically distinct lines of *Ae. aegypti*

To evaluate whether our observations of impaired blood digestion and increased ZIKV dissemination with antibiotic treatment are generalizable to *Ae. aegypti* from a different genetic background than Los Angeles, CA, we performed the similar analyses with *Ae. aegypti* obtained from Clovis, CA, where prior genome sequencing shows that the *Ae. aegypti* from Los Angeles and Clovis are genetically distinct (37), and were probably derived from separate independent introductions into California since 2013 when the species became established in the state. *Ae. aegypti* from Clovis were reared under the same antibiotic treatments as for Los Angeles mosquitoes. Blood digestion kinetics and ZIKV vector competence were then quantified in Clovis mosquitoes (**Figure 4A**). As observed for mosquitoes from Los Angeles, AbxA and AbxPA groups from Clovis demonstrated lower mean blood digestion relative to the No Abx group 2 dpf (K-W test with multiple comparisons, adjusted $P_{AbxPA\text{-}No\ Abx} = 0.0013$, adjusted $P_{AbxPA\text{-}AbxA} = 0.0271$) (**Figure 4B**). Also consistent with vector competence data from Los Angeles mosquitoes, the Clovis AbxPA group exhibited a marginally but not statistically significantly higher infection rate (34%) than both the Clovis AbxA (26%) and No Abx (15%) groups (Chi-square [χ^2] test, P = 0.106). The dissemination rate in the Clovis AbxPA group (26%) was

significantly higher than the No Abx (11%) and AbxA (10%) groups (χ^2, P = 0.04), although mean RNA levels in ZIKV-positive individuals were not different for any treatment (**Figure 4C**). These results from genetically distinct *Ae. aegypti* support the generalizability of our observations, where microbes augment blood digestion and reduce ZIKV susceptibility in *Ae. aegypti* from more than one genetic lineage.

Antibiotic treatment, blood ingestion, and ZIKV exposure influence the *Ae. aegypti* transcriptome

To identify gene expression differences underlying increased ZIKV susceptibility after antibiotic treatment of pupae and adults, we employed RNA-Seq analyses on pooled adult female *Ae. aegypti* from Los Angeles before bloodfeeding and 2 dpf. We also analyzed females that ingested blood only or ZIKV-spiked blood (**Figure 5A**). On average, 94.5% (min: 92.7, max: 95.7%) of reads from all samples aligned at least once to the Liverpool *Ae. aegypti* (LVP_WG) transcriptome. PCA showed tight clustering of mosquitoes prior to bloodfeeding distinct from mosquitoes that ingested blood with or without ZIKV (**Figure 5B**, **Figure S3A**). While most of the differences in gene expression related to bloodfeeding status, the presence of ZIKV in the bloodmeal also yielded differentially expressed genes (DEGs) for each antibiotic treatment. At baseline (without introduction of blood or ZIKV), 20 significant DEGs were found between AbxPA and No Abx (**Table S2**). The most downregulated gene in AbxPA relative to No Abx was uncharacterized (AAEL021374, adjusted P = 0.019), but other downregulated genes in AbxPA included membrane components (AAEL020586, adjusted P = 0; AAEL003626, adjusted P = 0.047) and ATP binding proteins (AAEL019793, adjusted P = 0.026; AAEL010711, adjusted P = 0.005). After bloodfeeding, over 1/3 of total genes in the *Ae. aegypti* genome were differentially expressed, consistent with other RNA-Seq studies (38). At 2 dpf, 7846 genes in No Abx, 9356 genes in AbxA, and 7846 genes in AbxPA were differentially expressed compared to sugar-fed

only. Among them, 6676 genes were shared among No Abx, AbxA, and AbxPA, representing an overwhelming majority of the total DEGs (**Figure S3B**). Between ZIKV-bloodfed and bloodfed only comparisons, differences were more visible. The AbxA and No Abx groups each had more DEGs between ZIKV-bloodfed and blood only individuals (No Abx: 1258 DEGs, AbxA: 1974) than AbxPA (62 DEGs) (**Figure 5C**, only DEGs that differed significantly across antibiotic treatments are shown [adjusted $P < 0.05$ by Wald test]). Most shared DEGs were between the AbxA and No Abx groups; AbxPA expressed a unique set of DEGs. Assignment of Kyoto Encyclopedia of Genes and Genomes (KEGG) pathway identity (IDs) to DEGs identified many unknown genes. Hypothetical protein products with no homology to genes with functional annotations were common (No Abx: 526, AbxA: 792, AbxPA: 29), as were genes involved in metabolic processes (No Abx: 371, AbxA: 599, AbxPA: 25) and thermogenesis (No Abx: 277, AbxA: 452, AbxPA: 9) (**Figure 5D**). Taken together, these data suggest that bloodfeeding has a larger effect than microbial exposure on *Ae. aegypti* gene expression. In ZIKV bloodfed mosquitoes, antibiotic treatment of both pupal and adult stages reduces differential gene expression more than treatment of adults only or no antibiotic treatment, indicating that pupal-derived microbes have a greater effect on the gene expression profile than adult-derived microbes.

Provided that microbes mediate immunomodulatory effects in mosquitoes (12,39,40), we theorized their presence could influence ZIKV susceptibility by modifying the expression of immune response pathways where some respond to both bacteria and viruses. We identified immunity-related DEGs across antibiotic-treated mosquitoes 2 dpf in the RNA-Seq data. Transcripts representing components of various immune pathways were accessioned from existing literature and used to filter the dataset before analyses of DEG profiles. Representative genes examined include regulators from Toll (41–43), RNAi (44–47), JAK-STAT (42,48,49), and Imd pathways (50,51), as well as general immune and immune-adjacent genes such as

hormones (52–55), antimicrobial peptides (AMPs) (49,56), reactive oxygen species (ROS) (57,58), and known DENV host factors (49,56). There were few DEGs demonstrating significant changes in transcript abundance in immune pathways between AbxA and AbxPA, No Abx and AbxA, or No Abx and AbxPA groups (**Figures 5E, S4**). Exceptions are gene CTP4H32 (AAEL007812, cytochrome p450 (38)) which was elevated in AbxA, and Unkn566 (AAEL000566, transmembrane protein in the JAK-STAT pathway (49)) which was elevated in AbxPA (**Figure 5E**). Comparison of immune genes between No Abx and AbxA and between No Abx and AbxPA, revealed a handful of genes that passed the statistical threshold; these are in the JAK-STAT pathway (Ukn566 between No Abx and AbxA; Ukn566 and Ukn7703 between No Abx and AbxPA) (**Figure S4**). These data suggest that gene expression changes after antibiotic treatment in ZIKV-exposed *Ae. aegypti* that show different susceptibility to disseminated infection are not related to known immune response pathways.

Gene ontology assignments reveal the role of microbiota in stimulating expression of protein digestion-associated genes in *Ae. aegypti* orally exposed to ZIKV

Given that RNA-Seq revealed no major differences in expression of immune response genes with antibiotic treatment, we next performed Gene Ontology (GO) analyses to predict enriched functions in non-immune associated DEGs. We identified DEGs displaying significant changes in abundance between the antibiotic treatments in mosquitoes that ingested ZIKV in blood or that ingested blood only. The AbxA and No Abx groups that ingested ZIKV in blood showed increased expression of genes enriched in general translation processes (AbxA: 125, adjusted $P < 10^{-10}$; No Abx: 127, adjusted $P < 10^{-20}$) and proteolysis (AbxA: 84, adjusted P = 0.0006; No Abx: 56, adjusted P = 0.015). In contrast, the AbxPA group showed few upregulated genes resulting in a lack of enriched functions (**Figure 6A**). Conversely, enrichments in genes downregulated in mosquitoes that ingested ZIKV in blood versus mosquitoes that ingested

blood only revealed that the ZIKV the AbxPA treatment group showed reduced transcript abundance for genes associated with DNA metabolism (8) and redox processes (4). AbxA and No Abx were depleted in genes for DNA replication (N=48 and 34, respectively) and DNA repair (N=18 and 2, respectively). All treatment groups that ingested blood with ZIKV compared to blood only exhibited downregulation of carbohydrate metabolism genes (AbxPA: N=8, adjusted P = 0.006; AbxA: N=6, adjusted P = 0.0002; No Abx: N=16, adjusted P = 0.017) (**Figure 6B**). These data suggest that microbiota during early ZIKV infection promote expression of genes associated with proteolysis and translation while downregulating genes relating to DNA synthesis.

The magnitude of change in DEGs in mosquitoes that ingested ZIKV in blood or blood only for each antibiotic treatment were also compared. Gene AAEL008117, the most depleted transcript in AbxA and No Abx groups (~20 $\log_2$-fold reduced), corresponds to nompC, a mechanosensitive ion channel that senses balance and touch in *Drosophila melanogaster* (59). The most common DEGs that changed in response to ZIKV exposure matched to proteolytic and PM-associated enzymes, including endopeptidases, collagenases, and dehydrogenases (60). Multiple serine-type endopeptidases were differentially expressed depending on antibiotic treatment (No Abx: AAEL001693, all three: AAEL008769, AbxA, and AbxPA: AAEL013284, AAEL001690) (**Figure 6C**). In addition, some vitellogenesis associated proteins were more enriched in antibiotic treated mosquitoes compared to the No Abx group (AbxA and AbxPA: AAEL014561 [vitelline membrane protein 15a-3], AbxPA: AAEL013027 [vitelline membrane protein 15a-1]). In AbxPA, the gene demonstrating the biggest reduction in transcript abundance corresponds to a m1 zinc metalloprotease (AAEL003012), showed increased expression in the No Abx group. Overall, GO analyses revealed *Ae. aegypti* with disrupted microbiota are deficient in genes that influence blood protein metabolism.

Discussion

In this study, we found that microbial exposure in two genetically distinct populations of *Ae. aegypti* facilitates midgut integrity and enhanced bloodmeal digestion. Together these effects reduce ZIKV infection of the midgut epithelium and result in less efficient dissemination out of the midgut (**Figure 7**). Reduced microbial colonization during both pupal and adult *Ae. aegypti* life stages, together with higher bloodmeal titers, produced the largest increases in susceptibility. These findings indicate that microbial exposure during the aqueous pupal stage of mosquito development is most important for conditioning susceptibility to ZIKV. These data show that larval microbial exposure confers developmental resistance to ZIKV dissemination out of the midgut by reinforcing midgut integrity after bloodfeeding.

Augmented rates of ZIKV infection and dissemination but not transmission in *Ae. aegypti* after antibiotic treatment suggest that microbial effects act at the midgut infection and escape barriers but not at salivary gland infection or escape barriers. Hematophagous feeding introduces a unique problem in that engorgement immensely distends the midgut. Midgut distention can result in breaches in the integrity of the epithelial barrier, presenting an opportunity for a virus ingested with blood to bypass infection of the epithelium. Prior studies detected bloodmeal-induced perforations in the midgut basal lamina, which do not fully recover after digestion, supporting a process where successive bloodmeals increase rates of ZIKV dissemination (61). Similar studies also found that ZIKV disseminates from the midgut after digestion is complete, which contrasts with the alphavirus CHIKV, which disseminates during digestion (62). Considering that we observed increased magnitude of and rate of bloodmeal digestion in ZIKV-exposed mosquitoes without antibiotics compared to antibiotic-treated pupae and adults, we envision a process where microbes accelerate digestion, decreasing the window of time the virus has to escape the bloodmeal, traverse the PM, and access the midgut epithelium, which

results in reduced ZIKV dissemination out of the midgut. We did not observe gross structural differences in the midgut epithelium with 10-40X DAPI and H&E staining, so we theorize that microbes do not impact midgut permeability by physically modifying the midgut epithelium. We acknowledge that increased midgut permeability may also allow for extracellular ZIKV traversion of the midgut epithelium, a process we did not measure in these studies.

Given that there are conserved elements of mosquito antiviral defenses and gut microbial homeostasis, including immune signaling and off-target suppression by ROS and AMPs (11,39), we were initially surprised that gene expression analyses did not detect differences in antiviral immune responses in response to antibiotic treatment. Rather, our RNA-Seq analyses confirm prior observations that show protein digestion and vitellogenesis dominate mosquito physiological processes after bloodfeeding (38). Our results are also similar to another transcriptomic study which found immense upregulation of proteases and trypsins 2 days post-ZIKV exposure (63). It stands to reason that blood digestion and vitellogenesis are hampered without the presence of microbial symbionts. Midgut symbionts may also indirectly reduce mosquito vector competence in multiple ways. These include supplementation of larval nutrition and development to increase mosquito fitness (9,64–67), stimulation of bloodfeeding behavior resulting in larger bloodmeals (although bloodmeal size differences were not observed in our studies) and increased nutrition (68), and regulation of midgut epithelial cell proliferation, where the physical microbe-midgut interface can block virus access to midgut infection (69) [although this may be pathogen specific as increased midgut infection has also been observed (21,70)].

Both microbes and ZIKV in bloodmeals resulted in increased blood digestion relative to antibiotic treated mosquitoes that ingested blood without virus. It is unclear why ZIKV enhances digestion; this may result from the virus modulating cell metabolism to benefit viral replication, a pattern shown for many viruses (71). In human cells, for example, infection with DENV elevates

glycolysis to meet cellular energy needs (72). Conceivably, a similar trend is true for ZIKV-infected mosquito midgut cells, where increased energy demand produced by viral infection is met by increasing blood metabolism. Absent ZIKV in the bloodmeal, antibiotic-treated mosquitoes exhibited digestive deficiencies during late digestion, defined here as beyond 2 dpf. Since blood ingestion is followed by rapid proliferation of midgut microbes that results from a heme-mediated reduction in ROS (73), the delayed digestion kinetics in antibiotic treated mosquitoes could be influenced by the near absence of microbes to promote digestion. Since blood digestion occurs in 2 phases where disparate enzymes dominate each phase (74), it is also possible that the digestive enzymes that have different efficiencies were differentially expressed across antibiotic treatments. We observed late trypsins and serine-type endopeptidases (enzyme types commonly found in the latter phase of digestion) (74–77) in all bloodfed antibiotic groups at 2 dpf; greater resolution of how digestion enzymes change over time is warranted to test this hypothesis. While over 300 serine protease-like proteins have been described in *Aedes spp.* (78,79), very few have been studied experimentally. One study implicated matrix metalloproteases and collagenase activity in degrading the basal lamina, which increased dissemination of CHIKV from the midgut (80). Our finding of a downregulated metalloprotease (AAEL003012) in mosquitoes with disrupted microbiota as pupae and adults, as well as an elevated serine collagenase precursor (AAEL007432) in mosquitoes that ingested ZIKV in blood supports a role of digestive enzymes in promoting arboviral dissemination. The potential interaction between blood protein metabolism and arboviral infection of mosquitoes warrants further study.

Whether blood digestion genes, including those that are differentially upregulated in mosquitoes exposed to antibiotics, can also modulate mosquito immune responses is currently unclear. A link between metabolism and immunity is possible (81). Some proteases have immune functions (82,83), including cleavage of proenzymes that activate the prophenoloxidase

pathway required for melanization (84). Metabolites influence and regulate immune pathways like Toll and Imd, and metabolic regulators balance microbial resistance and tolerance to gut symbionts in arthropods, including mosquitoes (63,81). In *Ae. aegypti*, blood-derived heme induces iron- and ROS-dependent signaling that also regulates immune genes, affecting DENV susceptibility (85). Metabolism of *Bacteroides* associates with elevated ZIKV susceptibility and conditions insecticide resistance (86), implicating a complex metabolic network that can also influence arbovirus susceptibility. Further investigation of the relationship between blood digestion and immunity could uncover novel determinants of mosquito vector competence.

Determining how microbes modulate the susceptibility of mosquitoes to arboviruses can help identify approaches to reduce transmission and decrease human disease. Microbial effects may also explain variability in vector competence across laboratories and geographic origins where each has different microbial communities (87), together with conventionally acknowledged factors like inbreeding during colonization (88,89). Our previous work, together with a growing body of mosquito microbiome studies, suggests that mosquito-microbe-virus interactions are environmentally variable and warrant investigation in more field-relevant contexts (14,18,67,90). A limitation of our studies is the use of a single microbial community and ZIKV strain. We acknowledge that disparate microbial species and community structures and other ZIKV strains could impact susceptibility differently. We also acknowledge that unculturable bacterial species could potentially play a role in mediating hemolytic activity that could have impacted blood digestion assays. Our use of antibiotics, which incompletely eliminates microbiota, most closely represents a dysbiotic phenotype. Newer tools including auxotrophic symbionts (91) and axenic mosquitoes (9) can be used to further investigate the metabolic roles of microbes in influencing arboviral infection of mosquitoes. Future studies of infection dynamics at the microbe-mosquito midgut interface could prove useful in reconciling disparate vector competence outcomes and discovering novel vector control approaches.

Acknowledgments We acknowledge Elise Ladouceur for helping interpret H&E imaging.

Funding Acknowledgements: This project was funded by the Training Grant Program of the Pacific Southwest Regional Center of Excellence for Vector-Borne Diseases funded by the U.S. Centers for Disease Control and Prevention (cooperative agreement 1U01CK000516). WL was also supported by the University of California, Davis, School of Veterinary Medicine Graduate Student Support Program. ALR was supported by the Coachella Valley Mosquito and Vector Control District. The funders had no role in study design, data collection and analysis, decision to publish, or preparation of the manuscript.

Author Contributions

Conceptualization: WL, LLC

Data Curation: WL, LKM, ETK

Formal Analysis: WL, LKM, ETK

Funding Acquisition: WL, LLC

Investigation: WL,

Methodology: WL, ALR, LLC, GMA

Project Administration: LLC

Resources: LLC

Supervision: LLC, GMA

Validation: WL

Visualization: WL, ALR, LLC

Writing-Original Draft: WL

Writing-Reviewing and Editing: WL, ALR, LLC, LKM, ETK, GMA

Figure 1. Antibiotic treatment of *Ae. aegypti* pupae and adults from Los Angeles, California, increases ZIKV susceptibility. A) Experimental design. Microbes from cemetery headstones were added to tap water during larvae rearing. Pupae in the antibiotic (Abx) groups were treated by adding an antibiotic cocktail to pupal water. No antibiotics (No Abx) groups received no antibiotics. Antibiotics were delivered orally in sugar to adult Abx (AbxA) groups; the No Abx group received sugar only. Mosquitoes from each group and life stage were sequenced to verify the efficacy of antibiotic treatment. Adult mosquitoes were presented with either of 2 doses of ZIKV spiked into bloodmeals, and ZIKV vector competence was assessed by measuring ZIKV RNA levels in bodies to determine infection, legs/wings to assess dissemination, and in saliva to measure transmission, which were measured as rates in cohorts and mean levels from individuals. **B) Antibiotic treatment reduces bacterial DNA in mosquitoes.** Bacteria was quantified in mosquitoes by 16S qPCR. Each point represents a single mosquito (N larvae, pupae, No Abx = 5; N AbxA, AbxPA = 10). 16S copies were normalized to the *Ae. aegypti* RPS17 gene. The limit of detection (LOD) was a 0.1 16S:RPS17 ratio; below this value, 16S was not detected. Statistical significance across all groups was determined by a Kruskal-Wallis test with multiple comparisons. **C) Vector competence of antibiotic treated mosquitoes for ZIKV.** Bar graphs show ZIKV infection, dissemination, and transmission rates in individual mosquitoes as determined by ZIKV RNA RT-qPCR. The summary table shows the same data as in the bar graphs. Rates were calculated as the number of bodies, legs/wings, or expectorates, respectively, that yielded at detectable ZIKV RNA, divided by the total number of individuals that ingested blood within a cohort. Statistical significance across all treatments was determined by Fisher's exact test. Vector competence experiments were conducted once. **D) Dose response to infection, dissemination, and transmission. Differences in** infection, dissemination, and transmission rates after ingestion of high versus low dose ZIKV bloodmeals (data from panel C). **ZIKV RNA levels in mosquito**

tissues after ingestion low (E) and **high (F) dose ZIKV-spiked bloodmeals**. Each dot shows the mean value for an individual mosquito based on triplicate measurements. The average LOD across all experiments was 3 copies per mosquito. For B, D, and E, geometric means are shown, and error bars show standard deviations among positive individuals. *Denotes $P < 0.05$ **denotes $P < 0.01$ Kolmogorov-Smirnov tests were used to compare RNA levels across antibiotic groups.

Figure 2. Antibiotic treatment modifies the structure and increases permeability and ZIKV infection of the *Ae. aegypti* midgut. A) Schematic of bloodfeeding experiment and sample preparation for immunofluorescence microscopy. Bloodmeal contained 1 µg dextran-FITC (green) and 3.3 x 10^6 PFU/mL ZIKV. Whole mosquitoes were harvested 0 days post-feed (dpf), cryosectioned, DAPI stained, and examined using fluorescence microscopy. Midguts from the same cohort were harvested at 2, and 3 dpf, and ZIKV antigen and DAPI-stained before fluorescence microscopy. **B) Antibiotic treatment disrupts regularity of DAPI staining in midgut epithelium.** Anterior-zoomed cross sections of whole, *Ae. aegypti* at 0 dpf about 30 to 60 minutes post-engorgement visualized at 10X magnification. **C) Antibiotic treatment of pupae and adults reduces midgut cell density.** Cell density was calculated as the number of cell nuclei (blue) per 100 µm length of gut. Each symbol represents one mosquito. **D) Dextran fluorescence quantification method** that was used to generate data in panel E. Fluorescence ratios were calculated in triplicate randomly selected areas in a single midgut slice, and each point represents the average of three slices in a single mosquito. **E) Antibiotic treatment of pupae and adults increases midgut permeability, evidenced by reduced relative dextran inside versus outside the gut lumen**. Dextran permeation was calculated as the ratio of fluorescence intensity inside the gut lumen to fluorescence intensity outside the gut lumen. Each symbol represents 9 measurements from one mosquito. Grey arrows indicate the individual represented in panel B. **F) Antibiotic treated pupae and adults have more ZIKV-infected**

midgut epithelial cells. The number of ZIKV-infected cells, as determined by ZIKV antigen staining, were counted for each ZIKV-positive midgut on 2 and 3 dpf. Data from both days is shown. Each symbol represents one mosquito. **G) Antibiotic treated ZIKV-positive midguts at 2 and 3 dpf.** Midguts examined under immunofluorescence at 10X magnification, at 2 and 3 dpf. Cell nuclei (blue) and ZIKV antigen (red) are shown with the combined (merged) channels. Images reflect representative observations for each antibiotic treatment. Lines show means and error bars show standard deviations. * Denotes P□<□0.05, ns is not significantly different at $p<0.05$.

Figure 3. Bloodmeal digestion kinetics in antibiotic treated *Ae. aegypti*. A) Experimental design for detection of hemoglobin in homogenized antibiotic treated mosquitoes that ingested blood with or without ZIKV. B) Despite ingesting equivalent bloodmeal sizes, antibiotic treatment reduces blood digestion in the absence of ZIKV at 2 and 3 dpf. *Ae. aegypti* that ingested blood (N: No Abx = 12, AbxA = 10, AbxPA = 15 per day) were assayed 0, 1, 2 and 3 dpf. **C) Despite ingesting equivalent bloodmeal sizes, antibiotic treatment reduces blood digestion with ZIKV at 1 and 2 dpf.** *Ae. aegypti* that ingested blood spiked with 2.1×10^6 PFU/mL ZIKV (N: No Abx = 18, AbxA = 12, AbxPA = 15 per day) were assayed 0, 1 and 2 dpf. **D) Mosquitoes not treated with antibiotics or treated only as adults that ingested ZIKV show increased blood digestion compared to mosquitoes treated with antibiotics as pupae and adults.** The bar graphs show the percent reduction in hemoglobin at 1 and 2 dpf compared to the 0 dpf, calculated for all Abx groups and between ZIKV challenged and unchallenged groups. Bars show mean and error bars indicate the standard deviation (raw values are shown in panels B and C). **E) Antibiotic treatment of pupae and adults results in higher ZIKV dissemination rates 3 dpf.** Legs and wings of individual bloodfed females from the same cohort were assayed by ZIKV RT-qPCR at three dpf. * Denotes P□<□0.05; ** denotes

P□<□0.01; ns is not significantly different. Each symbol in B, C and E shows the mean value for 1 mosquito.

Figure 4. Antibiotic treatment of *Ae. aegypti* pupae and adults from Clovis, California, decreases bloodmeal digestion and increases ZIKV susceptibility. A) Experimental design using the same assays as in Figures 1 and 3 applied to an *Ae. aegypti* colony from Clovis, CA. B) Despite ingesting equivalent bloodmeal sizes, antibiotic treatment reduces blood digestion with ZIKV at 2 dpf in Clovis mosquitoes. Error bars show the means and standard deviations (N = 15 for each treatment per day). **C) Antibiotic treatment of pupae and adults results in higher ZIKV dissemination rates at 14 dpf in Clovis mosquitoes.** ZIKV RNA levels from bloodfed Clovis *Ae. aegypti* at 14 dpf. Error bars denote the geometric means and standard deviations. The dotted line denotes the average LOD at 62 RNA copies/mosquito. The number of positives per number exposed is listed under the x-axis. Samples under the LOD included in rate measurements are not shown in panel C. (* is P□<□0.05; ** is P□<□0.01; ns is not significantly different). Each symbol in B and C shows the mean value for 1 mosquito.

Figure 5. Differentially expressed genes between antibiotic-treated adult *Ae. aegypti* females before and after a bloodmeal. A) Experimental design showing *Ae. aegypti* from Los Angeles, CA, pooling and RNA sequencing approach. For each antibiotic treatment and each bloodfeeding state, triplicate pools of 5 whole, legless mosquito bodies were RNA-extracted, pre-processed, and sequenced. **B) Transcriptome profile differs more by bloodmeal status than by antibiotic treatment.** PCA plot after variance stabilized transformation. Shapes indicate the bloodmeal status while colors represent the antibiotic treatments. Separate PCAs for individual variables, for ease of visibility, are shown in Figure S3. **C) ZIKV-responsive DEGs are shared among between *Ae. aegypti* not antibiotic-treated**

and antibiotic-treated as adults. Venn diagram of DEGs before and after bloodfeeding by *Ae. aegypti* for each antibiotic treatment. **D) DEGs correspond to metabolic processes, thermogenesis, and unknown genes for all antibiotic treatments.** KEGG Pathway ID assignment of DEGs in panel C. **E) DEGs between mosquitoes treated with antibiotics as pupae and adults compared to as adults only and ZIKV-bloodmeals or blood only do not correspond to known immune response genes.** Comparison of immune response gene expression between AbxA and AbxPA groups. Relative expression of select known and suspected immune-related genes from relevant literature (41–50,53–58). Expression is higher in AbxA if the $\log_2$-fold change is positive, while expression is higher in AbxPA if $\log_2$-fold change is negative. Points are considered significant (red) if the adjusted P value is < 0.01. Comparisons of the same genes between AbxA or AbxPA and the control treatment, No Abx, are shown in Figure S4.

Figure 6. Gene Ontology assignment of DEGs and identity of most enriched/depleted genes. Gene Ontology (GO) analysis of significant DEGs comparing antibiotic treatment mosquitoes that ingested ZIKV in bloodmeals versus blood only. **A) Upregulated GO hits for mosquitoes treated with antibiotics as adults or untreated primarily map to general translational processes and proteolysis.** Mosquitoes treated with antibiotics as pupae and adults demonstrate a reduced complement of proteolysis associated genes, and **B) GO enrichments in genes showing reduced transcript abundance for all antibiotic treatments primarily map to DNA synthesis and repair mechanisms.** GO terms for the DEGs (determined from Figures 5C-D) and their descriptions on the y-axis, and statistical significance (P-values, Fisher's exact test) of the GO term on the x-axis, with the exact number of DEGs within the colored circles. DEGs farther to the left (lower P-values) are more significant. **C) ZIKV-responsive DEGs demonstrating the highest magnitude fold change are distinct between AbxPA and No Abx treatment groups.** The top 10 upregulated and top 10

downregulated DEGs, by magnitude log_2-fold change for each antibiotic treatment. A positive log_2-fold change refers to more transcripts after a ZIKV-spiked bloodmeal, while a negative value refers to fewer transcripts. The right y-axis is the gene description from annotations retrieved from transcriptome metadata as well as VectorBase (32). Red text indicates the top genes shared between No Abx and AbxA. Purple text indicates the top genes shared between AbxPA and AbxA.

Figure 7. Schematic representation showing how microbes across mosquito life stages promote midgut permeability, increase bloodmeal digestion, and decrease ZIKV dissemination out of the *Ae. aegypti* midgut.

Figure S1. Histology of bloodfed female midguts. Cross sections of whole, bloodfed female *Ae. aegypti* along the median sagittal plane. H&E staining and bright field microscopy with a focus on the blood bolus perimeter was used to assess and identify potential structural artifacts during sample preparation that could confound immunofluorescence observations. Both 20X and 40X magnification of the same section are shown side-by-side. MG epithelium = midgut epithelium. PM region = peritrophic matrix region (where the fully formed PM would be seen). RBCs = red blood cells, from bloodmeal. BL side = basal laminal side.

Figure S2. Validation of hemoglobin colorimetric assay kit for bloodfed mosquitoes. A) Serial 1:2-fold dilutions of heparinized sheep blood were tested in parallel with the kit hemoglobin standard at the absorbance extremes of 560nm and 580nm. Lines indicate standard curves generated from linear regression that were used in the hemoglobin assays. **B)** Absorbance values of sheep blood hemoglobin after heat-treating at 60°C for 10 minutes in duplicates (rep = replicate).

Figure S3. DEGs from bloodfed antibiotic-treated mosquitoes that were not exposed to ZIKV. A) Individual PCA plots by a single variable representing the same data in Figure 5B. Shapes indicate the bloodmeal status while colors represent the antibiotic treatments. B) **DEGs between bloodfed and sugarfed *Ae. aegypti***.

Figure S4. Change in immune response gene expression across antibiotic treated groups of *Ae. aegypti*. A positive log_2-fold change indicates enrichment in AbxA or AbxPA, while a negative log_2-fold change indicates enrichment in No Abx.

Closest bacterial species to sequences from	E-value	Percent	Accession	Culture	Hemolytic

***Ae. aegypti* not treated with antibiotics**		**identity**	**Number**	**medium**	**activity?**
Elizabethkingia ursingii strain EM514-03	3.00E-124	99%	ON714894.1	R2A agar, sheep blood agar	no
Elizabethkingia bruuniana strain KMUH55	3.00E-124	99%	ON714884.1	R2A agar, sheep blood agar	no
Elizabethkingia miricola strain BM10	7.00E-56	85%	CP011059.1	R2A agar, sheep blood agar	no
Pseudomonas sp. MF0	3.00E-125	99%	AY331340.1	R2A agar	NA
Pseudacidovorax intermedius strain HMF4787	1.00E-124	99%	MN595029.1	R2A agar	NA
Salmonella clone (uncultured)	8.00E-126	99%	EF605247.1	R2A agar, sheep blood agar	no

Table S1. Bacterial isolates from adult *Ae.* aegypti that were not treated with antibiotics (No Abx). Cultured and isolated bacterial colonies from adult female *Ae. aegypti*, 3-5 dpe were Sanger sequenced at the V4 region of the 16S gene. Sequences were input into nucleotide BLAST, and the closest hits are reported. Hemolytic activity was tested by presence of ring of clearance around colonies (from lysed red blood cells) when cultured on sheep blood agar at 37°C. NA indicates hemolytic activity was not evaluated.

Gene	**Log_2Fold Change**	**Adjusted P**	**GO accession**	**GO term**	**Gene description**

AAEL021374	-4.99	0.019	NA	NA	NA
AAEL020586	-2.88	0.000	GO:0016020	membrane	NA
AAEL003626	-1.27	0.047	GO:0016021	integral component of membrane	sodium/chloride dependent amino acid transporter
AAEL019793	-1.00	0.026	GO:0005524	ATP binding	NA
AAEL010711	-1.00	0.005	GO:0005524	ATP binding	eph receptor tyrosine kinase
AAEL020123	-0.95	0.040	NA	NA	NA
AAEL019444	-0.87	0.022	GO:0003723	RNA binding	NA
AAEL004715	-0.86	0.041	GO:0008285	negative regulation of cell population proliferation	b-cell translocation protein
AAEL017280	-0.85	0.040	GO:0003677	DNA binding	NA
AAEL007041	-0.83	0.033	GO:0005509	calcium ion binding	low-density lipoprotein receptor (ldl)
AAEL027453	1.49	0.019	GO:0004550	nucleoside diphosphate kinase activity	NA
AAEL012832	1.88	0.026	GO:0031902	late endosome membrane	cytochrome B561
AAEL000384	3.58	0.000	GO:0055085	transmembrane transport	vesicular acetylcholine transporter
AAEL012340	4.56	0.026	GO:0016788	hydrolase activity, acting on ester bonds	lipase 1 precursor
AAEL029026	8.16	0.026	NA	NA	NA
AAEL014561	8.47	0.040	GO:0005576	extracellular region	NA

Table S2. DEGs between sugarfed *Ae. aegypti* without antibiotics or antibiotic treated as pupae and adults. A negative Log_2fold-change refers to downregulation in AbxPA vs No Abx, while a positive Log_2fold-change refers to upregulation in AbxPA vs No Abx.

References

1. Winokur OC, Main BJ, Nicholson J, Barker CM. Impact of temperature on the extrinsic incubation period of Zika virus in *Aedes aegypti*. Althouse B, editor. PLoS Negl Trop Dis. 2020 Mar 18;14(3):e0008047.
2. Onyango MG, Bialosuknia SM, Payne AF, Mathias N, Kuo L, Vigneron A, et al. Increased temperatures reduce the vectorial capacity of *Aedes* mosquitoes for Zika virus. Emerg Microbes Infect. 2020 Jan 1;9(1):67–77.
3. Kain MP, Skinner EB, Athni TS, Ramirez AL, Mordecai EA, van den Hurk AF. Not all mosquitoes are created equal: A synthesis of vector competence experiments reinforces virus associations of Australian mosquitoes. Brackney DE, editor. PLoS Negl Trop Dis. 2022 Oct 4;16(10):e0010768.
4. Boyer S, Calvez E, Chouin-Carneiro T, Diallo D, Failloux AB. An overview of mosquito vectors of Zika virus. Microbes Infect. 2018 Dec;20(11–12):646–60.
5. Coon KL, Brown MR, Strand MR. Mosquitoes host communities of bacteria that are essential for development but vary greatly between local habitats. Mol Ecol. 2016 Nov;25(22):5806–26.
6. Coon KL, Vogel KJ, Brown MR, Strand MR. Mosquitoes rely on their gut microbiota for development. Mol Ecol. 2014 Jun;23(11):2727–39.
7. Scolari F, Casiraghi M, Bonizzoni M. *Aedes* spp. and Their Microbiota: A Review. Front Microbiol. 2019 Sep 4;10:2036.
8. Mancini MV, Damiani C, Accoti A, Tallarita M, Nunzi E, Cappelli A, et al. Estimating bacteria diversity in different organs of nine species of mosquito by next generation sequencing. BMC Microbiol. 2018 Dec;18(1):126.
9. Correa MA, Matusovsky B, Brackney DE, Steven B. Generation of axenic *Aedes aegypti* demonstrate live bacteria are not required for mosquito development. Nat Commun [Internet]. 2018 Dec [cited 2019 Mar 1];9(1). Available from: http://www.nature.com/articles/s41467-018-07014-2

10. Gaio A de O, Gusmão DS, Santos AV, Berbert-Molina MA, Pimenta PF, Lemos FJ. Contribution of midgut bacteria to blood digestion and egg production in *Aedes aegypti* (diptera: culicidae) (L.). Parasit Vectors. 2011;4(1):105.
11. El-Sherbini M, Hamed A, Abdeltawab M. The Mosquito Microbiota Interplay in Immune Signalling, Vector competence, and Control Prospects. Egypt Acad J Biol Sci G Microbiol. 2022 Mar 25;14(1):101–12.
12. Guégan M, Zouache K, Démichel C, Minard G, Tran Van V, Potier P, et al. The mosquito holobiont: fresh insight into mosquito-microbiota interactions. Microbiome. 2018 Dec;6(1):49.
13. Engel P, Moran NA. The gut microbiota of insects – diversity in structure and function. FEMS Microbiol Rev. 2013 Sep;37(5):699–735.
14. Louie W, Coffey LL. Microbial Composition in Larval Water Enhances *Aedes aegypti* Development but Reduces Transmissibility of Zika Virus. Einav S, editor. mSphere. 2021 Dec 22;6(6):e00687-21.
15. Hegde S, Khanipov K, Albayrak L, Golovko G, Pimenova M, Saldaña MA, et al. Microbiome interaction networks and community structure from laboratory-reared and field-collected *Aedes aegypti*, *Aedes albopictus*, and *Culex quinquefasciatus* mosquito vectors. Front Microbiol [Internet]. 2018 Sep 10 [cited 2019 Feb 13];9. Available from: https://www.frontiersin.org/article/10.3389/fmicb.2018.02160/full
16. Onyango MG, Payne AF, Stout J, Dieme C, Kuo L, Kramer LD, et al. Potential for transmission of *Elizabethkingia anophelis* by *Aedes albopictus* and the role of microbial interactions in Zika vector competence. bioRxiv. 2020;
17. Möhlmann TWR, Vogels CBF, Göertz GP, Pijlman GP, ter Braak CJF, te Beest DE, et al. Impact of Gut Bacteria on the Infection and Transmission of Pathogenic Arboviruses by Biting Midges and Mosquitoes. Microb Ecol. 2020 Oct;80(3):703–17.

18. Giraud É, Varet H, Legendre R, Sismeiro O, Aubry F, Dabo S, et al. Mosquito-bacteria interactions during larval development trigger metabolic changes with carry-over effects on adult fitness. Mol Ecol. 2022 Jan 3;mec.16327.
19. Brown LD, Shapiro LLM, Thompson GA, Estévez-Lao TY, Hillyer JF. Transstadial immune activation in a mosquito: Adults that emerge from infected larvae have stronger antibacterial activity in their hemocoel yet increased susceptibility to malaria infection. Ecol Evol. 2019 May;9(10):6082–95.
20. Rodgers FH, Gendrin M, Wyer CAS, Christophides GK. Microbiota-induced peritrophic matrix regulates midgut homeostasis and prevents systemic infection of malaria vector mosquitoes. Dimopoulos G, editor. PLOS Pathog. 2017 May 17;13(5):e1006391.
21. Wu P, Sun P, Nie K, Zhu Y, Shi M, Xiao C, et al. A gut commensal bacterium promotes mosquito permissiveness to arboviruses. Cell Host Microbe. 2019 Jan;25(1):101-112.e5.
22. Deng SQ, Zou WH, Li DL, Chen JT, Huang Q, Zhou LJ, et al. Expression of *Bacillus thuringiensis* toxin Cyt2Ba in the entomopathogenic fungus *Beauveria bassiana* increases its virulence towards *Aedes* mosquitoes. Kittayapong P, editor. PLoS Negl Trop Dis. 2019 Jul 15;13(7):e0007590.
23. Silva-Filha MHNL. Bacterial Toxins Active against Mosquitoes: Mode of Action and Resistance. 2021;37.
24. Klindworth A, Pruesse E, Schweer T, Peplies J, Quast C, Horn M, et al. Evaluation of general 16S ribosomal RNA gene PCR primers for classical and next-generation sequencing-based diversity studies. Nucleic Acids Res. 2013 Jan 1;41(1):e1–e1.
25. Dzaki N, Ramli KN, Azlan A, Ishak IH, Azzam G. Evaluation of reference genes at different developmental stages for quantitative real-time PCR in *Aedes aegypti*. Sci Rep. 2017 Apr;7(1):43618.

26. Main BJ, Nicholson J, Winokur OC, Steiner C, Riemersma KK, Stuart J, et al. Vector competence of *Aedes aegypti*, *Culex tarsalis*, and *Culex quinquefasciatus* from California for Zika virus. Turell MJ, editor. PLoS Negl Trop Dis. 2018 Jun 21;12(6):e0006524.
27. Lemos D, Stuart JB, Louie W, Singapuri A, Ramírez AL, Watanabe J, et al. Two Sides of a Coin: a Zika Virus Mutation Selected in Pregnant Rhesus Macaques Promotes Fetal Infection in Mice but at a Cost of Reduced Fitness in Nonpregnant Macaques and Diminished Transmissibility by Vectors. J Virol [Internet]. 2020 Nov 23 [cited 2020 Dec 14];94(24). Available from: https://jvi.asm.org/content/94/24/e01605-20
28. Talyuli OAC, Oliveira JHM, Bottino-Rojas V, Silveira GO, Alvarenga PH, Kantor AM, et al. The *Aedes aegypti* peritrophic matrix controls arbovirus vector competence through HPx1, a heme–induced peroxidase [Internet]. Microbiology; 2022 Jun [cited 2022 Sep 13]. Available from: http://biorxiv.org/lookup/doi/10.1101/2022.06.02.494599
29. Schindelin J, Arganda-Carreras I, Frise E, Kaynig V, Longair M, Pietzsch T, et al. Fiji: an open-source platform for biological-image analysis. Nat Methods. 2012 Jul;9(7):676–82.
30. Martin M. Cutadapt removes adapter sequences from high-throughput sequencing reads. EMBnet.journal. 2011 May 2;17(1):10.
31. Andrews S. FastQC: A Quality Control Tool for High Throughput Sequence Data [Online] [Internet]. 2010. Available from: http://www.bioinformatics.babraham.ac.uk/projects/fastqc/
32. Giraldo-Calderón GI, Emrich SJ, MacCallum RM, Maslen G, Dialynas E, Topalis P, et al. VectorBase: an updated bioinformatics resource for invertebrate vectors and other organisms related with human diseases. Nucleic Acids Res. 2015 Jan 28;43(D1):D707–13.
33. Langmead B, Salzberg SL. Fast gapped-read alignment with Bowtie 2. Nat Methods. 2012 Apr;9(4):357–9.
34. Love MI, Huber W, Anders S. Moderated estimation of fold change and dispersion for RNA-seq data with DESeq2. 2014;21.

35. Adrian Alexa JR. topGO: Enrichment Analysis for Gene Ontology [Internet]. Bioconductor; 2022 [cited 2022 Oct 24]. Available from: https://bioconductor.org/packages/topGO
36. R Core Team. R: A Language and Environment for Statistical Computing [Internet]. Vienna, Austria: R Foundation for Statistical Computing; 2022. Available from: https://www.R-project.org/
37. Lee Y, Schmidt H, Collier TC, Conner WR, Hanemaaijer MJ, Slatkin M, et al. Genome-wide divergence among invasive populations of *Aedes aegypti* in California. BMC Genomics. 2019 Dec;20(1):204.
38. Bonizzoni M, Dunn WA, Campbell CL, Olson KE, Dimon MT, Marinotti O, et al. RNA-seq analyses of blood-induced changes in gene expression in the mosquito vector species, *Aedes aegypti*. BMC Genomics. 2011 Dec;12(1):82.
39. Caragata EP. Curious entanglements: interactions between mosquitoes, their microbiota, and arboviruses. Curr Opin Virol. 2019;11.
40. Ramirez JL, Souza-Neto J, Torres Cosme R, Rovira J, Ortiz A, Pascale JM, et al. Reciprocal tripartite interactions between the *Aedes aegypti* midgut microbiota, innate immune system and dengue virus influences vector competence. O'Neill SL, editor. PLoS Negl Trop Dis. 2012 Mar 6;6(3):e1561.
41. Chowdhury A, Modahl CM, Tan ST, Wong Wei Xiang B, Missé D, Vial T, et al. JNK pathway restricts DENV2, ZIKV and CHIKV infection by activating complement and apoptosis in mosquito salivary glands. Dimopoulos G, editor. PLOS Pathog. 2020 Aug 10;16(8):e1008754.
42. Xi Z, Ramirez JL, Dimopoulos G. The *Aedes aegypti* Toll pathway controls dengue virus infection. Schneider DS, editor. PLoS Pathog. 2008 Jul 4;4(7):e1000098.
43. Zhao L, Alto BW, Jiang Y, Yu F, Zhang Y. Transcriptomic analysis of *Aedes aegypti* innate immune system in response to ingestion of chikungunya virus. Int J Mol Sci. 2019 Jun 27;20(13):3133.

44. Olmo RP, Ferreira AGA, Izidoro-Toledo TC, Aguiar ERGR, de Faria IJS, de Souza KPR, et al. Control of dengue virus in the midgut of *Aedes aegypti* by ectopic expression of the dsRNA-binding protein Loqs2. Nat Microbiol. 2018 Dec;3(12):1385–93.
45. Gestuveo RJ, Parry R, Dickson LB, Lequime S, Sreenu VB, Arnold MJ, et al. Mutational analysis of *Aedes aegypti* Dicer 2 provides insights into the biogenesis of antiviral exogenous small interfering RNAs. McGraw EA, editor. PLOS Pathog. 2022 Jan 6;18(1):e1010202.
46. Sánchez-Vargas I, Scott JC, Poole-Smith BK, Franz AWE, Barbosa-Solomieu V, Wilusz J, et al. Dengue virus type 2 infections of *Aedes aegypti* are modulated by the mosquito's RNA interference pathway. Rice CM, editor. PLoS Pathog. 2009 Feb 13;5(2):e1000299.
47. Almire F, Terhzaz S, Terry S, McFarlane M, Gestuveo RJ, Szemiel AM, et al. Sugar feeding protects against arboviral infection by enhancing gut immunity in the mosquito vector Aedes aegypti. Goodman AG, editor. PLOS Pathog. 2021 Sep 2;17(9):e1009870.
48. Souza-Neto JA, Sim S, Dimopoulos G. An evolutionary conserved function of the JAK-STAT pathway in anti-dengue defense. Proc Natl Acad Sci. 2009 Oct 20;106(42):17841–6.
49. Jupatanakul N, Sim S, Angleró-Rodríguez YI, Souza-Neto J, Das S, Poti KE, et al. Engineered *Aedes aegypti* JAK/STAT pathway-mediated immunity to dengue virus. Olson KE, editor. PLoS Negl Trop Dis. 2017 Jan 12;11(1):e0005187.
50. Feng Y, Chen L, Gao L, Dong L, Wen H, Song X, et al. Rapamycin inhibits pathogen transmission in mosquitoes by promoting immune activation. Strand MR, editor. PLOS Pathog. 2021 Feb 24;17(2):e1009353.
51. Barletta ABF, Nascimento-Silva MCL, Talyuli OAC, Oliveira JHM, Pereira LOR, Oliveira PL, et al. Microbiota activates IMD pathway and limits Sindbis infection in *Aedes aegypti*. Parasit Vectors. 2017 Dec;10(1):103.

52. Ferreira PG, Tesla B, Horácio ECA, Nahum LA, Brindley MA, de Oliveira Mendes TA, et al. Temperature Dramatically Shapes Mosquito Gene Expression With Consequences for Mosquito–Zika Virus Interactions. Front Microbiol. 2020 Jun 12;11:901.
53. Hyde J, Correa MA, Hughes GL, Steven B, Brackney DE. Limited influence of the microbiome on the transcriptional profile of female *Aedes aegypti* mosquitoes. Sci Rep. 2020 Dec;10(1):10880.
54. Shin D, Kang S, Smartt CT. Profiling Transcripts of Vector Competence between Two Different *Aedes aegypti* Populations in Florida. Viruses. 2020 Jul 29;12(8):823.
55. Colpitts TM, Cox J, Vanlandingham DL, Feitosa FM, Cheng G, Kurscheid S, et al. Alterations in the *Aedes aegypti* transcriptome during infection with West Nile, dengue and yellow fever viruses. Rice CM, editor. PLoS Pathog. 2011 Sep 1;7(9):e1002189.
56. Sim S, Jupatanakul N, Ramirez JL, Kang S, Romero-Vivas CM, Mohammed H, et al. Transcriptomic profiling of diverse *Aedes aegypti* strains reveals increased basal-level immune activation in dengue virus-refractory populations and identifies novel virus-vector molecular interactions. Ribeiro JMC, editor. PLoS Negl Trop Dis. 2013 Jul 4;7(7):e2295.
57. Oliveira JHM, Talyuli OAC, Goncalves RLS, Paiva-Silva GO, Sorgine MHF, Alvarenga PH, et al. Catalase protects *Aedes aegypti* from oxidative stress and increases midgut infection prevalence of dengue but not Zika. Apperson C, editor. PLoS Negl Trop Dis. 2017 Apr 5;11(4):e0005525.
58. Wang JM, Cheng Y, Shi ZK, Li XF, Xing LS, Jiang H, et al. *Aedes aegypti* HPX8C modulates immune responses against viral infection. Dumonteil E, editor. PLoS Negl Trop Dis. 2019 Apr 15;13(4):e0007287.
59. Wang Y, Guo Y, Li G, Liu C, Wang L, Zhang A, et al. The push-to-open mechanism of the tethered mechanosensitive ion channel NompC. eLife. 2021 Jun 8;10:e58388.

60. Whiten SR, Ray WK, Helm RF, Adelman ZN. Characterization of the adult *Aedes aegypti* early midgut peritrophic matrix proteome using LC-MS. Weiss BL, editor. PLOS ONE. 2018 Mar 23;13(3):e0194734.
61. Armstrong PM, Ehrlich H, Bransfield A, Warren JL, Pitzer VE, Brackney DE. Successive bloodmeals enhance virus dissemination within mosquitoes and increase transmission potential [Internet]. Microbiology; 2018 Jan [cited 2019 Dec 9]. Available from: http://biorxiv.org/lookup/doi/10.1101/246306
62. Cui Y, Grant DG, Lin J, Yu X, Franz AWE. Zika Virus Dissemination from the Midgut of *Aedes aegypti* is Facilitated by Bloodmeal-Mediated Structural Modification of the Midgut Basal Lamina. Viruses. 2019 Nov 14;11(11):1056.
63. Etebari K, Hegde S, Saldaña MA, Widen SG, Wood TG, Asgari S, et al. Global Transcriptome Analysis of *Aedes aegypti* Mosquitoes in Response to Zika Virus Infection. Fernandez-Sesma A, editor. mSphere. 2017 Dec 27;2(6):mSphere.00456-17, e00456-17.
64. Valzania L, Martinson VG, Harrison RE, Boyd BM, Coon KL, Brown MR, et al. Both living bacteria and eukaryotes in the mosquito gut promote growth of larvae. Bartholomay LC, editor. PLoS Negl Trop Dis. 2018 Jul 6;12(7):e0006638.
65. Minard G, Tran FH, Tran Van V, Fournier C, Potier P, Roiz D, et al. Shared larval rearing environment, sex, female size and genetic diversity shape *Ae. albopictus* bacterial microbiota. Oliveira PL, editor. PLOS ONE. 2018 Apr 11;13(4):e0194521.
66. Coon KL, Valzania L, McKinney DA, Vogel KJ, Brown MR, Strand MR. Bacteria-mediated hypoxia functions as a signal for mosquito development. Proc Natl Acad Sci. 2017 Jul 3;114(27):E5362–9.
67. Dickson LB, Jiolle D, Minard G, Moltini-Conclois I, Volant S, Ghozlane A, et al. Carryover effects of larval exposure to different environmental bacteria drive adult trait variation in a mosquito vector. Sci Adv. 2017 Aug;3(8):e1700585.

68. Kozlova EV, Hegde S, Roundy CM, Golovko G, Saldana MA, Hart CE, et al. Microbial interactions in the mosquito gut determine Serratia colonization and blood feeding propensity. [Internet]. Microbiology; 2020 Apr [cited 2020 Nov 2]. Available from: http://biorxiv.org/lookup/doi/10.1101/2020.04.14.039701
69. Taracena ML, Bottino-Rojas V, Talyuli OAC, Walter-Nuno B, Oliveira JHM, Wells MB, et al. Regulation of midgut cell proliferation impacts *Aedes aegypti* susceptibility to dengue virus. 2018;21.
70. Apte-Deshpande AD, Paingankar MS, Gokhale MD, Deobagkar DN. *Serratia odorifera* mediated enhancement in susceptibility of *Aedes aegypti* for chikungunya virus. Indian J Med Res. 2014;139(5):762–8.
71. Goodwin CM, Xu S, Munger J. Stealing the Keys to the Kitchen: Viral Manipulation of the Host Cell Metabolic Network. Trends Microbiol. 2015 Dec;23(12):789–98.
72. Fontaine KA, Sanchez EL, Camarda R, Lagunoff M. Dengue Virus Induces and Requires Glycolysis for Optimal Replication. Sandri-Goldin RM, editor. J Virol. 2015 Feb 15;89(4):2358–66.
73. Oliveira JHM, Gonçalves RLS, Lara FA, Dias FA, Gandara ACP, Menna-Barreto RFS, et al. Blood meal-derived heme decreases ROS levels in the midgut of *Aedes aegypti* and allows proliferation of intestinal microbiota. Schneider DS, editor. PLoS Pathog. 2011 Mar 17;7(3):e1001320.
74. Felix CR, Betschart B, Billingsley PF, Freyvogel TA. Post-feeding induction of trypsin in the midgut of *Aedes aegypti* L. (Diptera: Culicidae) is separable into two cellular phases. Insect Biochem. 1991 Jan;21(2):197–203.
75. Barillas-Mury C, Graf R, Hagedorn HH, Wells MA. cDNA and deduced amino acid sequence of a blood meal-induced trypsin from the mosquito, *Aedes aegypti*. Insect Biochem. 1991 Jan;21(8):825–31.

76. Kalhok. SE, Tabak LM, Prosser DE, Brook W, Downe AER, White BN. Isolation, sequencing and characterization of two cDNA clones coding for trypsin-like enzymes from the midgut of *Aedes aegypti*. Insect Mol Biol. 1993 Oct;2(2):71–9.
77. Li X, Yang J, Pu Q, Peng X, Xu L, Liu S. Serine hydroxymethyltransferase controls blood-meal digestion in the midgut of *Aedes aegypti* mosquitoes. Parasit Vectors. 2019 Dec;12(1):460.
78. Brackney DE, Isoe J, W.C. B, Zamora J, Foy BD, Miesfeld RL, et al. Expression profiling and comparative analyses of seven midgut serine proteases from the yellow fever mosquito, *Aedes aegypti*. J Insect Physiol. 2010 Jul;56(7):736–44.
79. Saboia-Vahia L, Cuervo P, Borges-Veloso A, de Souza NP, Britto C, Dias-Lopes G, et al. The midgut of *Aedes albopictus* females expresses active trypsin-like serine peptidases. Parasit Vectors. 2014 Dec;7(1):253.
80. Dong S, Balaraman V, Kantor AM, Lin J, Grant DG, Held NL, et al. Chikungunya virus dissemination from the midgut of *Aedes aegypti* is associated with temporal basal lamina degradation during bloodmeal digestion. Powers AM, editor. PLoS Negl Trop Dis. 2017 Sep 29;11(9):e0005976.
81. Samaddar S, Marnin L, Butler LR, Pedra JHF. Immunometabolism in Arthropod Vectors: Redefining Interspecies Relationships. Trends Parasitol. 2020 Oct;36(10):807–15.
82. Borovsky D. Biosynthesis and Control of Mosquito Gut Proteases. IUBMB Life Int Union Biochem Mol Biol Life. 2003 Aug 1;55(8):435–41.
83. Gorman MJ, Paskewitz SM. Serine proteases as mediators of mosquito immune responses. Insect Biochem Mol Biol. 2001 Mar;31(3):257–62.
84. El Moussawi L, Nakhleh J, Kamareddine L, Osta MA. The mosquito melanization response requires hierarchical activation of non-catalytic clip domain serine protease homologs. Dimopoulos G, editor. PLOS Pathog. 2019 Nov 25;15(11):e1008194.

85. Bottino-Rojas V, Talyuli OAC, Jupatanakul N, Sim S, Dimopoulos G, Venancio TM, et al. Heme Signaling Impacts Global Gene Expression, Immunity and Dengue Virus Infectivity in *Aedes aegypti*. Missirlis F, editor. PLOS ONE. 2015 Aug 14;10(8):e0135985.
86. Arévalo-Cortés A, Damania A, Granada Y, Zuluaga S, Mejia R, Triana-Chavez O. Association of Midgut Bacteria and Their Metabolic Pathways with Zika Infection and Insecticide Resistance in Colombian Aedes aegypti Populations. Viruses. 2022 Oct 6;14(10):2197.
87. Kauffman EB, Kramer LD. Zika Virus Mosquito Vectors: Competence, Biology, and Vector Control. J Infect Dis. 2017 Dec 16;216(suppl_10):S976–90.
88. Powell JR, Evans BR. How Much Does Inbreeding Reduce Heterozygosity? Empirical Results from *Aedes aegypti*. Am J Trop Med Hyg. 2017 Jan 11;96(1):157–8.
89. Soma DD, Maïga H, Mamai W, Bimbile-Somda NS, Venter N, Ali AB, et al. Does mosquito mass-rearing produce an inferior mosquito? Malar J. 2017 Dec;16(1):357.
90. Coatsworth H, Caicedo PA, Van Rossum T, Ocampo CB, Lowenberger C. The composition of midgut bacteria in *Aedes aegypti* (Diptera: Culicidae) that are naturally susceptible or refractory to dengue viruses. J Insect Sci [Internet]. 2018 Nov 1 [cited 2019 Feb 13];18(6). Available from: https://academic.oup.com/jinsectscience/article/doi/10.1093/jisesa/iey118/5228717
91. Romoli O, Schönbeck JC, Hapfelmeier S, Gendrin M. Production of germ-free mosquitoes via transient colonisation allows stage-specific investigation of host–microbiota interactions. Nat Commun. 2021 Dec;12(1):942.

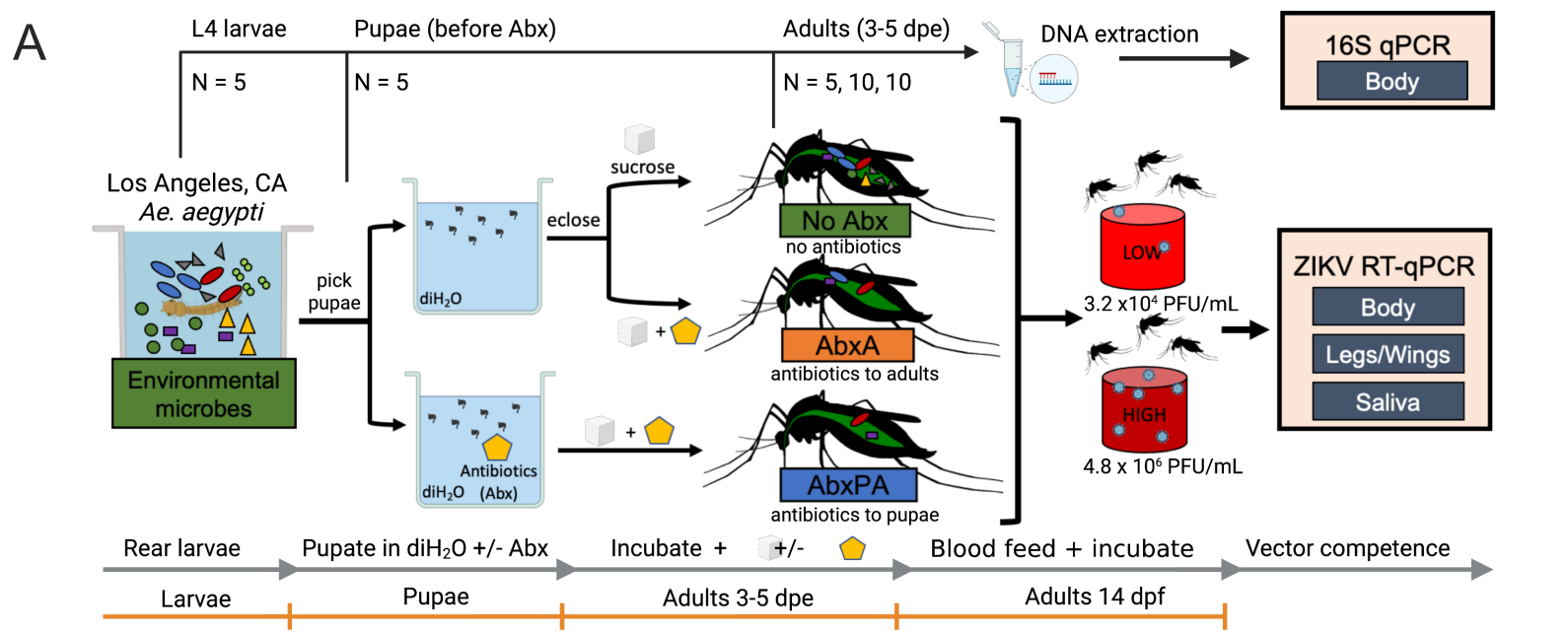

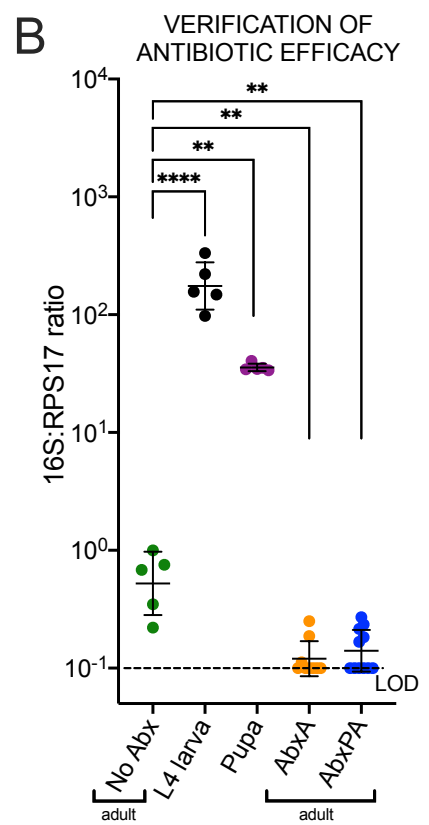

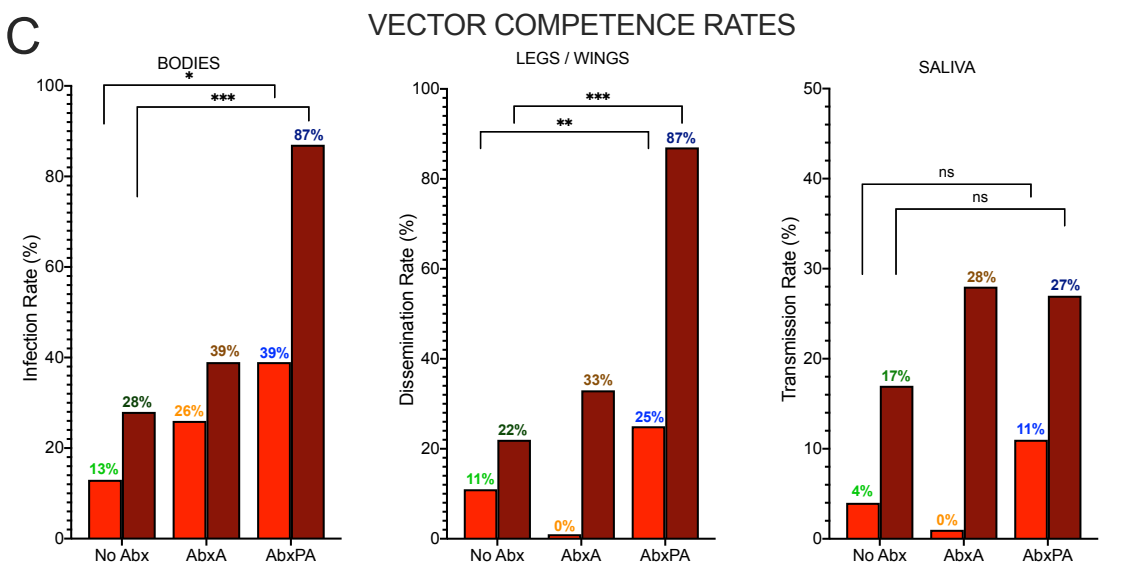

Generation	Group	ZIKV dose (PFU/mL)	Infection Rate	Dissemination Rate	Transmission Rate	Infection Sig. (P)	Dissemination Sig. (P)	Transmission Sig. (P)
F_{20}	No Abx	3.2×10^4	13% (6/45)	11% (5/45)	4% (2/45)	0.0398	0.0081	0.1376
	AbxA		26% (9/34)	0% (0/34)	0% (0/34)			
	AbxPA		39% (11/28)	25% (7/28)	11% (3/28)			
F_{22}	No Abx	4.8×10^6	28% (5/18)	22% (4/18)	17% (3/18)	< 0.0001	< 0.0001	0.6767
	AbxA		39% (7/18)	33% (6/18)	28% (5/18)			
	AbxPA		87% (26/30)	87% (26/30)	27% (8/30)			

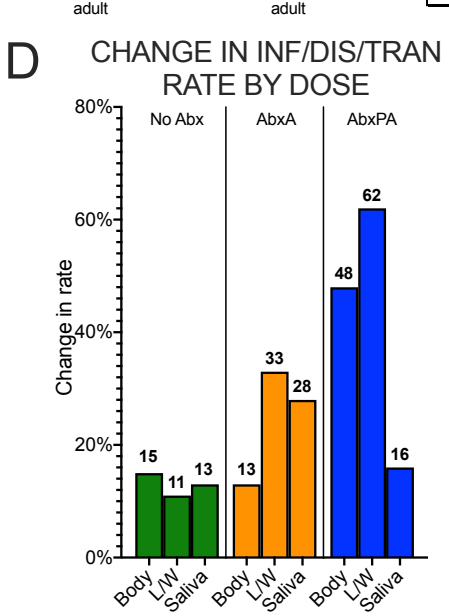

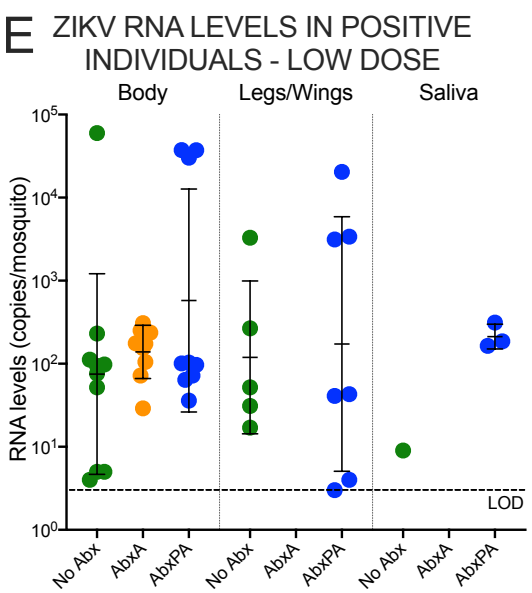

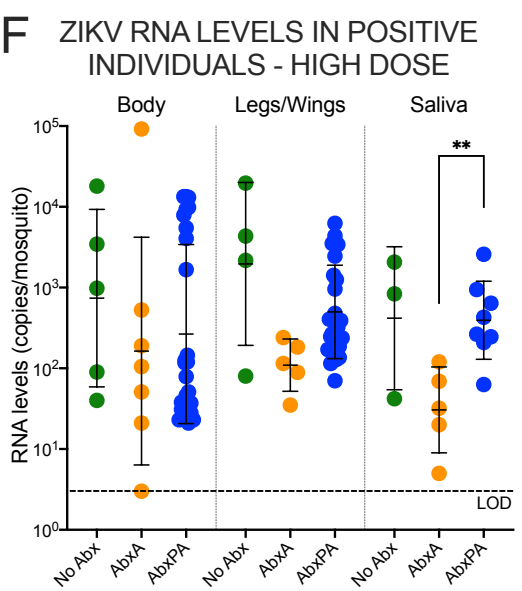

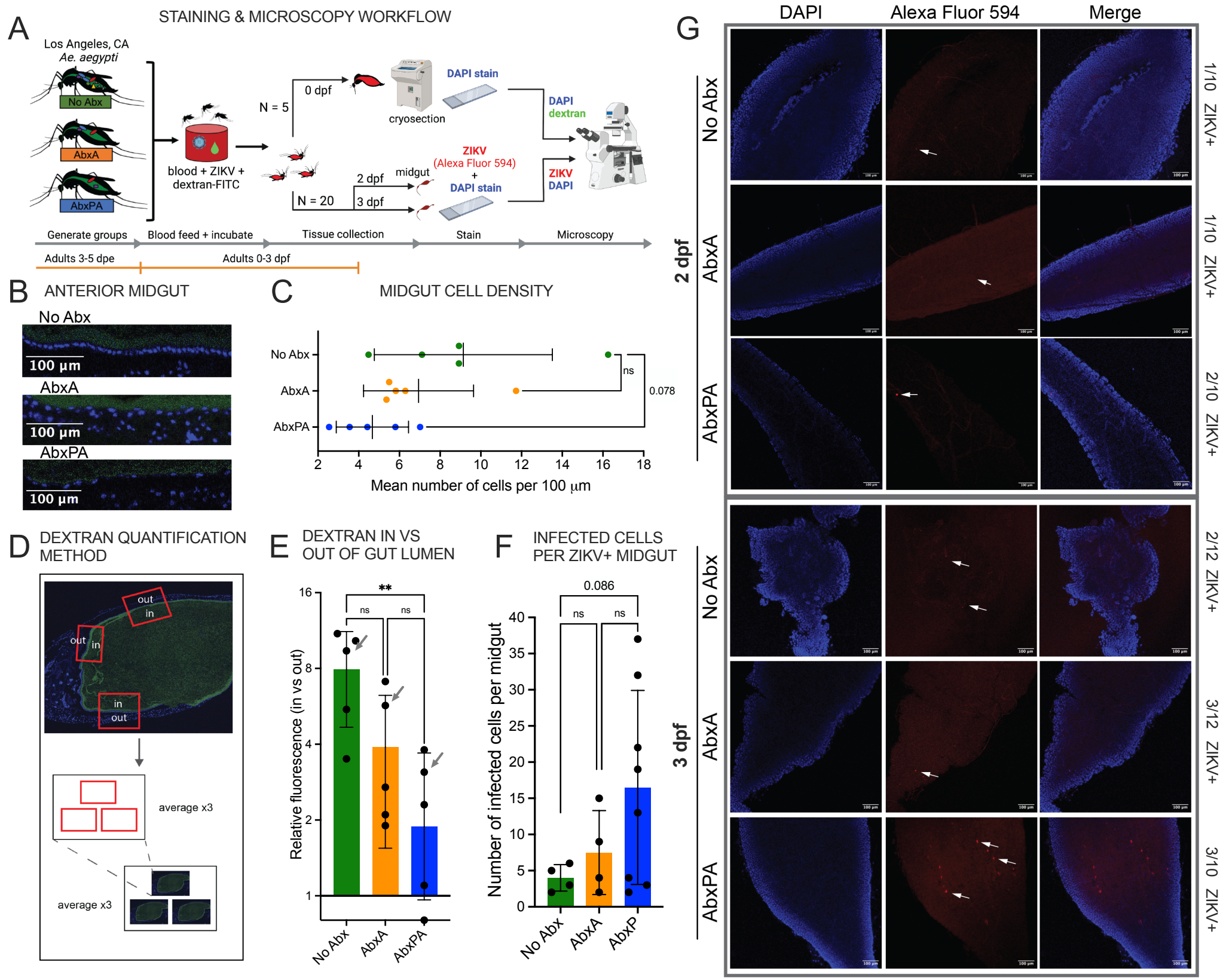
A
STAINING & MICROSCOPY WORKFLOW
Los Angeles, CA
Ae. aegypti
No Abx
AbxA
AbxPA
blood + ZIKV + dextran-FITC
N = 5
0 dpf
cryosection
DAPI stain
DAPI dextran
N = 20
2 dpf
3 dpf
midgut
ZIKV (Alexa Fluor 594) + DAPI stain
ZIKV DAPI
Generate groups
Blood feed + incubate
Tissue collection
Stain
Microscopy
Adults 3-5 dpe
Adults 0-3 dpf
B
ANTERIOR MIDGUT
No Abx
AbxA
AbxPA
100 µm
C
MIDGUT CELL DENSITY
No Abx
AbxA
AbxPA
ns
0.078
Mean number of cells per 100 µm
D
DEXTRAN QUANTIFICATION METHOD
out
in
average x3
E
DEXTRAN IN VS OUT OF GUT LUMEN
**
ns
Relative fluorescence (in vs out)
No Abx
AbxA
AbxPA
F
INFECTED CELLS PER ZIKV+ MIDGUT
0.086
Number of infected cells per midgut
No Abx
AbxA
AbxP
G
DAPI
Alexa Fluor 594
Merge
2 dpf
3 dpf
1/10 ZIKV+
2/10 ZIKV+
2/12 ZIKV+
3/12 ZIKV+
3/10 ZIKV+

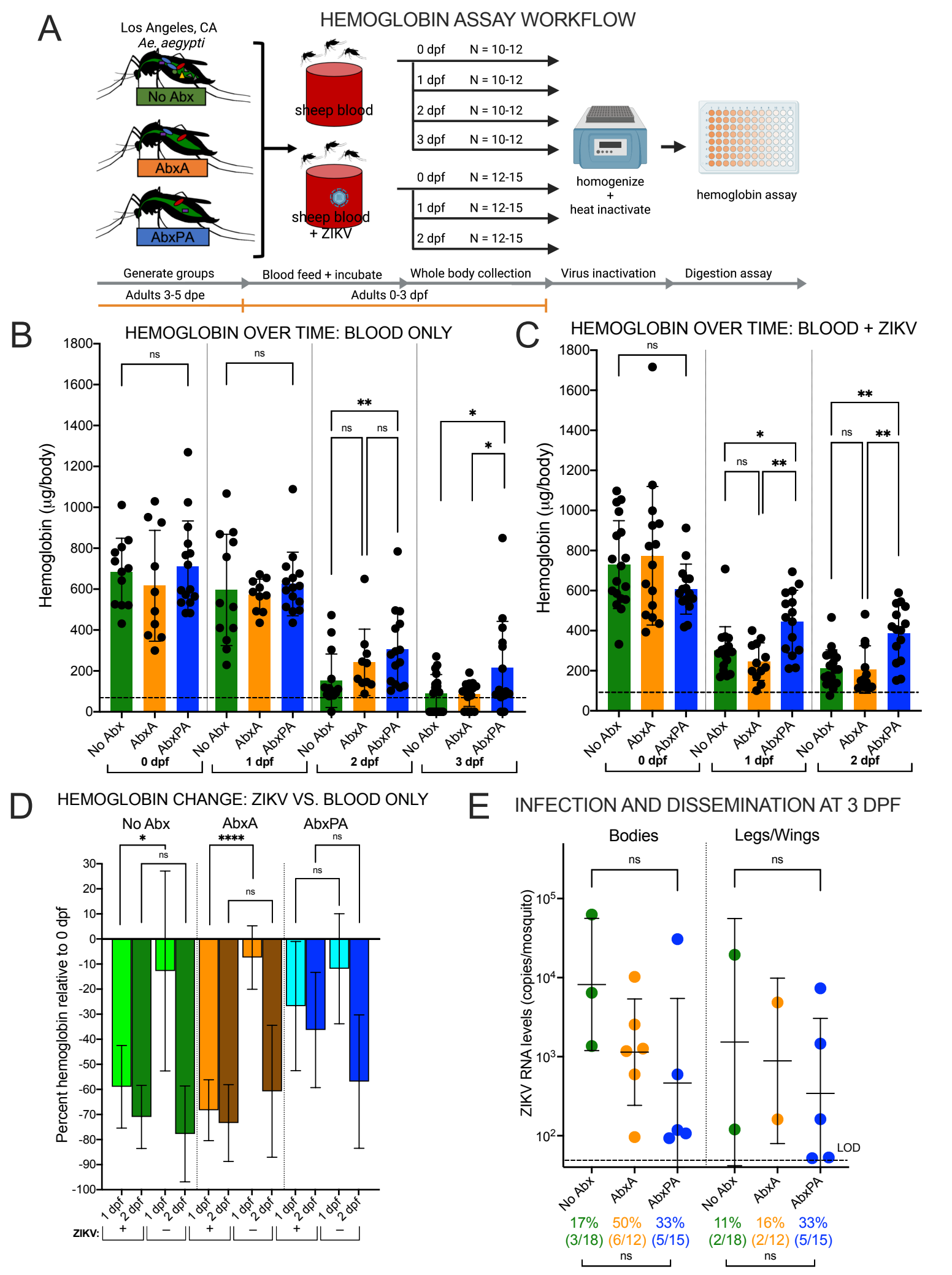
A
HEMOGLOBIN ASSAY WORKFLOW
Los Angeles, CA
Ae. aegypti
No Abx
AbxA
AbxPA
sheep blood
sheep blood + ZIKV
0 dpf N = 10-12
1 dpf N = 10-12
2 dpf N = 10-12
3 dpf N = 10-12
0 dpf N = 12-15
1 dpf N = 12-15
2 dpf N = 12-15
homogenize + heat inactivate
hemoglobin assay
Generate groups
Blood feed + incubate
Whole body collection
Virus inactivation
Digestion assay
Adults 3-5 dpe
Adults 0-3 dpf
B
HEMOGLOBIN OVER TIME: BLOOD ONLY
Hemoglobin (µg/body)
0 dpf
1 dpf
2 dpf
3 dpf
C
HEMOGLOBIN OVER TIME: BLOOD + ZIKV
D
HEMOGLOBIN CHANGE: ZIKV VS. BLOOD ONLY
Percent hemoglobin relative to 0 dpf
ZIKV:
E
INFECTION AND DISSEMINATION AT 3 DPF
Bodies
Legs/Wings
ZIKV RNA levels (copies/mosquito)
LOD
17% (3/18)
50% (6/12)
33% (5/15)
11% (2/18)
16% (2/12)
33% (5/15)

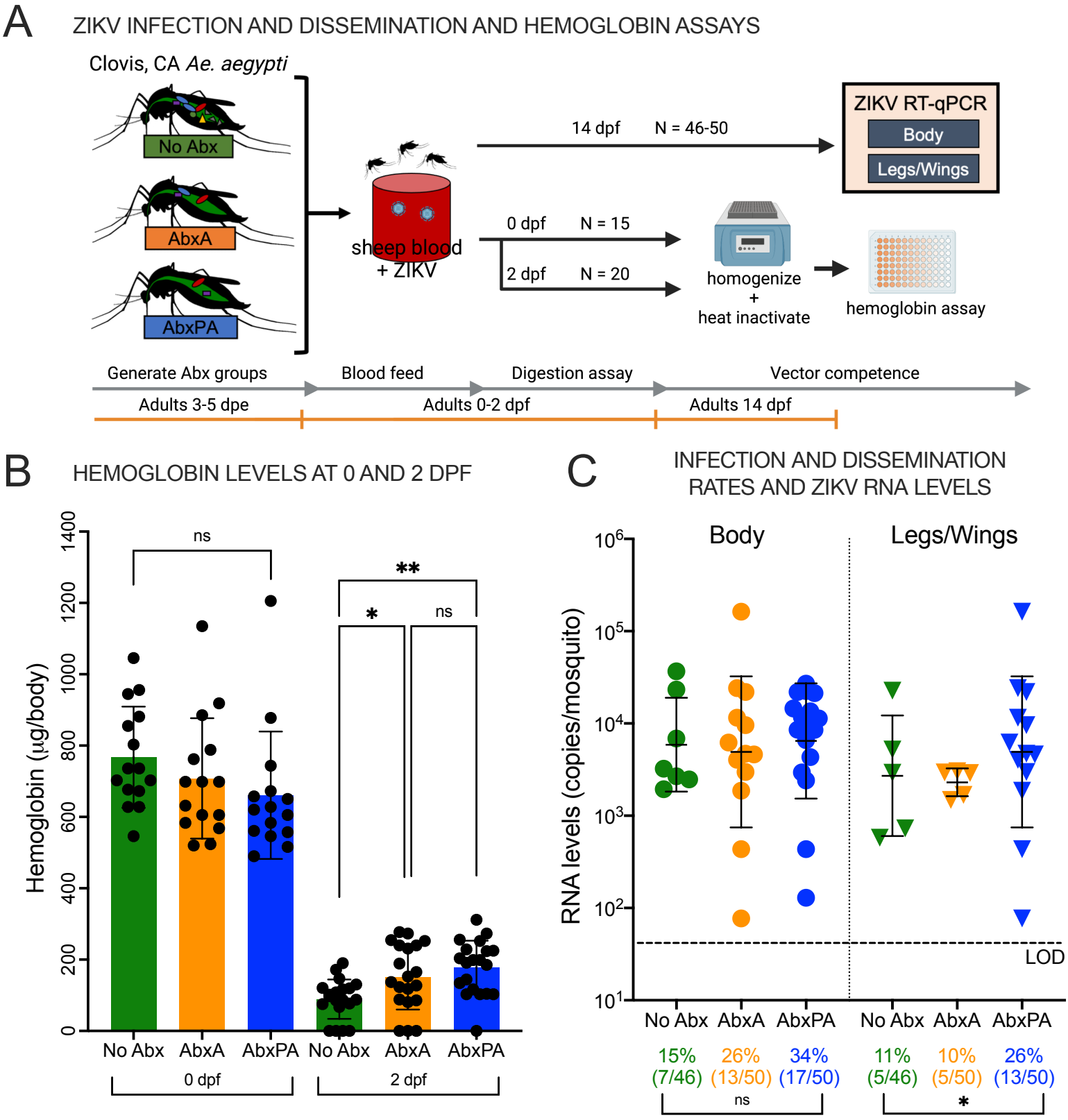
A
ZIKV INFECTION AND DISSEMINATION AND HEMOGLOBIN ASSAYS
Clovis, CA Ae. aegypti
No Abx
AbxA
AbxPA
sheep blood
+ ZIKV
14 dpf
N = 46-50
ZIKV RT-qPCR
Body
Legs/Wings
0 dpf
N = 15
2 dpf
N = 20
homogenize
+
heat inactivate
hemoglobin assay
Generate Abx groups
Blood feed
Digestion assay
Vector competence
Adults 3-5 dpe
Adults 0-2 dpf
Adults 14 dpf
B
HEMOGLOBIN LEVELS AT 0 AND 2 DPF
Hemoglobin (µg/body)
0
200
400
600
800
1000
1200
1400
ns
**
*
ns
No Abx
AbxA
AbxPA
No Abx
AbxA
AbxPA
0 dpf
2 dpf
C
INFECTION AND DISSEMINATION
RATES AND ZIKV RNA LEVELS
Body
Legs/Wings
RNA levels (copies/mosquito)
10^6
10^5
10^4
10^3
10^2
10^1
LOD
No Abx
AbxA
AbxPA
No Abx
AbxA
AbxPA
15%
(7/46)
26%
(13/50)
34%
(17/50)
11%
(5/46)
10%
(5/50)
26%
(13/50)
ns
*

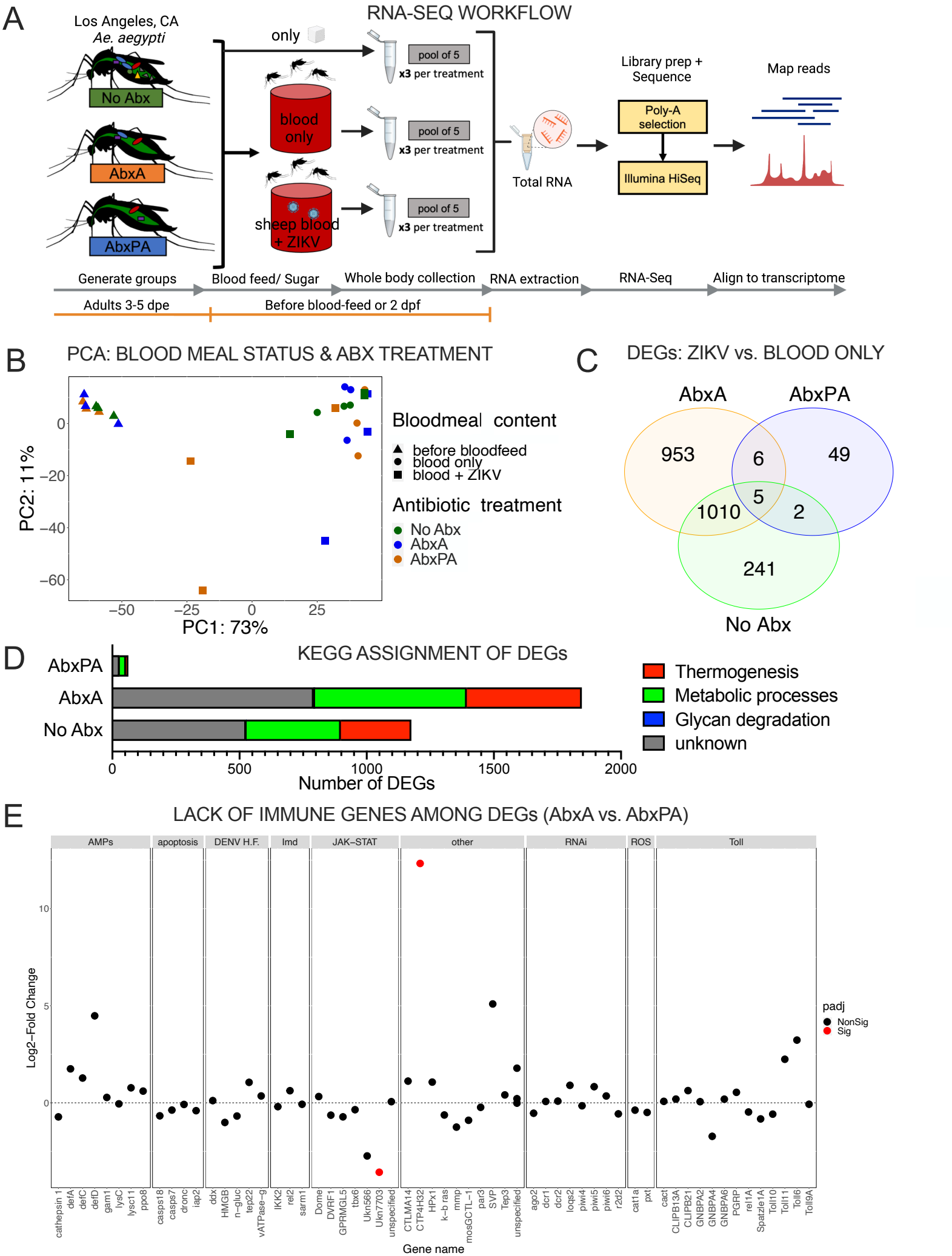
A
RNA-SEQ WORKFLOW
Los Angeles, CA
Ae. aegypti
No Abx
AbxA
AbxPA
only
blood only
sheep blood + ZIKV
pool of 5
x3 per treatment
Total RNA
Library prep + Sequence
Poly-A selection
Illumina HiSeq
Map reads
Generate groups
Blood feed/ Sugar
Whole body collection
RNA extraction
RNA-Seq
Align to transcriptome
Adults 3-5 dpe
Before blood-feed or 2 dpf
B
PCA: BLOOD MEAL STATUS & ABX TREATMENT
PC2: 11%
PC1: 73%
Bloodmeal content
before bloodfeed
blood only
blood + ZIKV
Antibiotic treatment
No Abx
AbxA
AbxPA
C
DEGs: ZIKV vs. BLOOD ONLY
AbxA
AbxPA
No Abx
953
6
49
5
1010
2
241
D
KEGG ASSIGNMENT OF DEGs
AbxPA
AbxA
No Abx
Number of DEGs
Thermogenesis
Metabolic processes
Glycan degradation
unknown
E
LACK OF IMMUNE GENES AMONG DEGs (AbxA vs. AbxPA)
AMPs
apoptosis
DENV H.F.
Imd
JAK–STAT
other
RNAi
ROS
Toll
Log2–Fold Change
padj
NonSig
Sig
cathepsin 1
defA
defC
defD
gam1
lysC
lysc11
ppo8
casps18
casps7
dronc
iap2
ddx
HMGB
n–gluc
tep22
vATPase–g
IKK2
rel2
sarm1
Dome
DVRF1
GPRMGL5
tbx6
Ukn566
Ukn7703
unspecified
CTLMA14
CTP4H32
HPx1
k–b ras
mmp
mosGCTL–1
par3
SVP
Tep3
unspecified
ago2
dcr1
dcr2
loqs2
piwi4
piwi5
piwi6
r2d2
cat1a
pxt
cact
CLIPB13A
CLIPB21
GNBPA2
GNBPA4
GNBPA6
PGRP
rel1A
Spatzle1A
Toll10
Toll11
Toll6
Toll9A
Gene name

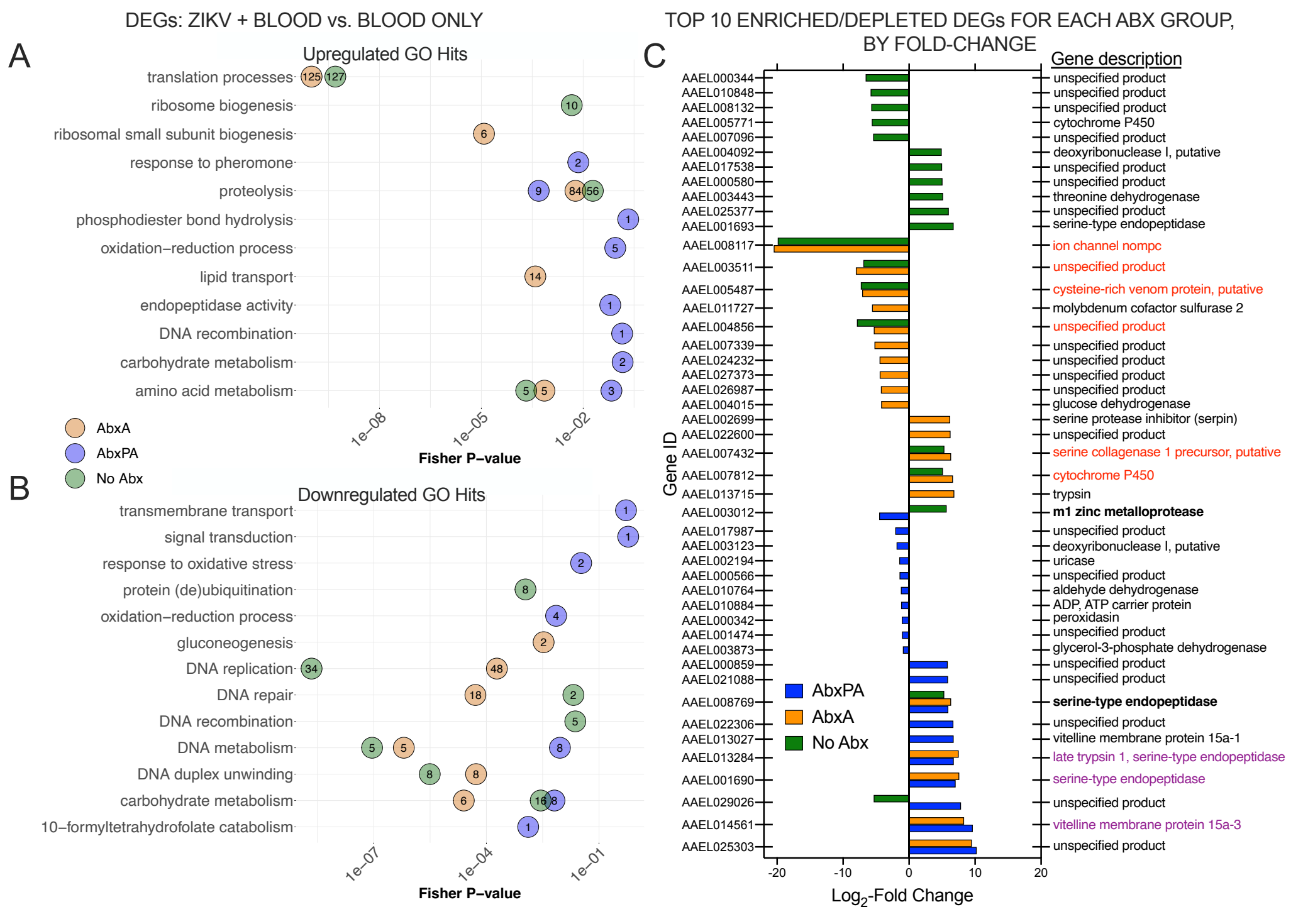
DEGs: ZIKV + BLOOD vs. BLOOD ONLY
A
Upregulated GO Hits
translation processes
ribosome biogenesis
ribosomal small subunit biogenesis
response to pheromone
proteolysis
phosphodiester bond hydrolysis
oxidation−reduction process
lipid transport
endopeptidase activity
DNA recombination
carbohydrate metabolism
amino acid metabolism
1e−08
1e−05
1e−02
Fisher P−value
AbxA
AbxPA
No Abx
B
Downregulated GO Hits
transmembrane transport
signal transduction
response to oxidative stress
protein (de)ubiquitination
oxidation−reduction process
gluconeogenesis
DNA replication
DNA repair
DNA recombination
DNA metabolism
DNA duplex unwinding
carbohydrate metabolism
10−formyltetrahydrofolate catabolism
1e−07
1e−04
1e−01
Fisher P−value
TOP 10 ENRICHED/DEPLETED DEGs FOR EACH ABX GROUP, BY FOLD-CHANGE
C
Gene description
Gene ID
AAEL000344 unspecified product
AAEL010848 unspecified product
AAEL008132 unspecified product
AAEL005771 cytochrome P450
AAEL007096 unspecified product
AAEL004092 deoxyribonuclease I, putative
AAEL017538 unspecified product
AAEL000580 unspecified product
AAEL003443 threonine dehydrogenase
AAEL025377 unspecified product
AAEL001693 serine-type endopeptidase
AAEL008117 ion channel nompc
AAEL003511 unspecified product
AAEL005487 cysteine-rich venom protein, putative
AAEL011727 molybdenum cofactor sulfurase 2
AAEL004856 unspecified product
AAEL007339 unspecified product
AAEL024232 unspecified product
AAEL027373 unspecified product
AAEL026987 unspecified product
AAEL004015 glucose dehydrogenase
AAEL002699 serine protease inhibitor (serpin)
AAEL022600 unspecified product
AAEL007432 serine collagenase 1 precursor, putative
AAEL007812 cytochrome P450
AAEL013715 trypsin
AAEL003012 m1 zinc metalloprotease
AAEL017987 unspecified product
AAEL003123 deoxyribonuclease I, putative
AAEL002194 uricase
AAEL000566 unspecified product
AAEL010764 aldehyde dehydrogenase
AAEL010884 ADP, ATP carrier protein
AAEL000342 peroxidasin
AAEL001474 unspecified product
AAEL003873 glycerol-3-phosphate dehydrogenase
AAEL000859 unspecified product
AAEL021088 unspecified product
AAEL008769 serine-type endopeptidase
AAEL022306 unspecified product
AAEL013027 vitelline membrane protein 15a-1
AAEL013284 late trypsin 1, serine-type endopeptidase
AAEL001690 serine-type endopeptidase
AAEL029026 unspecified product
AAEL014561 vitelline membrane protein 15a-3
AAEL025303 unspecified product
AbxPA
AbxA
No Abx
-20
-10
0
10
20
Log2-Fold Change

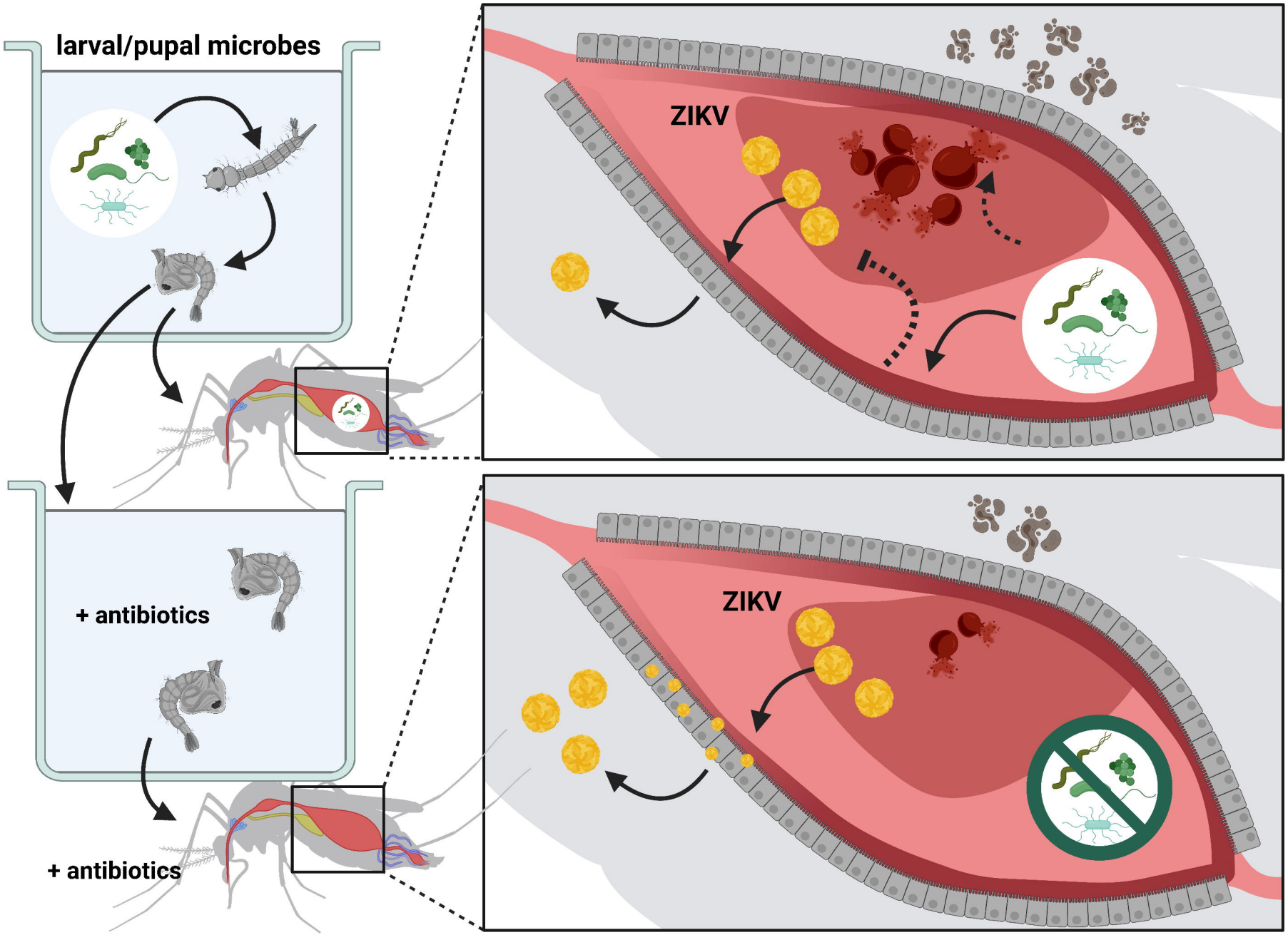
larval/pupal microbes
ZIKV
+ antibiotics
ZIKV
+ antibiotics